CHALMERS

Test Vehicle for Regenerative Braking Emulation

Master's Thesis in the Master's program Automotive Engineering

HORACE LAI AND DAVID MADÅS

Department of Applied Mechanics
Division of Vehicle Engineering and Autonomous Systems
CHALMERS UNIVERSITY OF TECHNOLOGY
Göteborg, Sweden 2011
Master's Thesis 2011:10

MASTER'S THESIS 2011:10

Test Vehicle for Regenerative Braking Emulation

Master's Thesis in the Master's Program Automotive Engineering

Horace Lai and David Madås

Department of Applied Mechanics
Division of Vehicle Engineering and Autonomous Systems
CHALMERS UNIVERSITY OF TECHNOLOGY
Göteborg, Sweden 2011

Test Vehicle for Regenerative Braking Emulation
Master's Thesis in the Master's Program Automotive Engineering
HORACE LAI AND DAVID MADÅS

Master's Thesis 2011:10
ISSN 1652-8557
Department of Applied Mechanics
Division of Vehicle Engineering and Autonomous Systems
Chalmers University of Technology
SE-412 96 Göteborg
Sweden
Telephone: + 46 (0)31-772 1000

Cover:
Test vehicle during calibration of torque measurement wheels.

Reproservice / Department of Applied Mechanics
Göteborg, Sweden 2011

Test Vehicle for Regenerative Braking Emulation

Master's Thesis in the Master's Program Automotive Engineering
Horace Lai and David Madås
Department of Applied Mechanics
Division of Vehicle Engineering and Autonomous Systems
Chalmers University of Technology

ABSTRACT

The recent increase in global environmental concern drives the development of fuel saving vehicle technologies. A way to save fuel is to recuperate kinetic energy into a usable form for propulsive purposes, which is known as regenerative (regen) braking. However, regen braking also influences the vehicle stability and the driver's perception of the brake system. The impact of the human factor imposes the use of a test vehicle during development of regen braking strategies. The production of a regen braking test vehicle was initiated by SAAB as part of their Hybrid Vehicles and eAWD project and conducted by this master thesis.

The main use of the test vehicle is to analyze the limitations of additive regen braking, where additional electric motor brake torque is applied on top of the standard brake torque. Additive braking allows the original brake system to be retained, saving production costs while giving fuel consumption improvements. Also, it facilitates the transition process to hybrid vehicles.

The perfect test vehicle for regen braking would possess one electric motor for each wheel and the necessary ancillaries. However, this vehicle project would have an intrinsic high level of packaging complexity, cost and engineering time. To overcome these negative aspects, another concept was conceived, in which a second hydraulic brake system is controlled to emulate electric motors. Electric motors are emulated in the sense that the friction brake wheel torque is equal to that produced by an electric motor. This concept consists of extra calipers clamping the original rotors, an Electro-Hydraulic Brake (EHB) unit delivering brake pressure and a dSpace onboard computer running the test program.

Simulink models of a generic electric driveline were developed to emulate the behavior of regen braking. The models include the battery, electric motor, power converter, and motor controller. These models calculate the wheel torque to be applied, which needs to be converted to a pressure value for the EHB unit. A brake model was developed to calculate the pressure, taking into account the temperature which affects the friction coefficient between the pad and disc.

A hardware-in-the-loop rig was used for calibration of the brake model. Additionally, torque measuring wheels were installed on the test vehicle to calibrate the software and to validate the performance of the vehicle.

The result of this thesis is an easy-to-use test vehicle which can conduct experiments dealing with additive regen braking, as well as any brake based vehicle system. For engineers to get started quickly, an example case study and a user manual are provided. The result of the research utilizing the test vehicle will be seen in the next generation SAAB hybrid vehicles.

Key words: Regenerative braking, test vehicle, electric vehicles, brake system.

Contents

Preface

In this thesis, a test vehicle for emulation of regenerative braking has been developed and tested. The work was carried out from mid September 2010 to early April 2011. The development of the test vehicle was initiated by SAAB Automobile as part of their Hybrid Vehicles and eAWD project. Although most of the work was done at SAAB Automobile, some tests were carried out at Chalmers University of Technology at the Department of Electrical Engineering. The collaboration with Chalmers University of Technology also extends to plans of building a similar test vehicle for use at Chalmers.

Supervisors of the project have been Gunnar Olsson at SAAB Automobile and Peter Stavered at eAAM. Examiner is Mathias Lidberg at the Department of Applied Mechanics, Division of Vehicle Engineering and Autonomous Systems at Chalmers University of Technology. The authors would like to thank Gunnar Olsson, Peter Stavered and Mathias Lidberg for their invaluable guidance throughout the project as well as Klas Olsson and Carl Sandberg for their efforts on the Chalmers HIL-rig. The help from all consulted engineers and workshop workers at SAAB Automobile is highly appreciated, especially the great efforts of Kjell Carlsson, Klas-Göran Ryrlén and Jouko Kähkönen.

Trollhättan April 2011

Horace Lai and David Madås

Notations

Roman upper case letters

A	Area
B	Magnetic flux density
E	Induced electric motor force voltage (e.m.f)
F	Force
I	Electric current
Q	Heat
R	Electrical resistance
T	Torque
ΔT	Temperature difference
V	Voltage

Roman lower case letters

c	Specific heat
h	Convection coefficient
k	Thermal conductivity
k_e	E.m.f constant
k_t	Torque constant
l	Length
m	Mass
μ	Friction
n	Number of caliper pistons
ω	Rotational velocity
p	pressure
r	Radius
v	Velocity

1 Introduction

1.1 Background

The recent increase in global environmental concern drives the development of fuel saving vehicle technologies. A way to save fuel is to recuperate kinetic energy into a usable form for propulsion, which is known as regenerative (regen) braking. There are substantial amounts of energy to be saved by using regen braking systems, even though it varies with the vehicle type and driving situation (Wicks and Donnelly). However, regen braking also influences the vehicle stability and the driver's perception of the brake system. The impact of the human factor necessitates the use of a test vehicle during development of regen braking strategies. The production of a regen braking test vehicle was therefore initiated by SAAB as part of their Hybrid Vehicles and eAWD project and conducted by this master thesis.

1.2 Problem definition

A way of recuperating brake energy is to use an electric motor in generator mode, providing brake torque while charging a battery. An electric machine is usually unable to replicate the functionality of friction brakes, as the wheel torque capability is generally less than for friction brakes. Therefore, a second friction based brake system should be retained. Mixing friction braking and regen braking is challenging, since the maximum brake torque of an electric machine varies with vehicle speed. Additionally, regen braking might influence the stability of the vehicle. These factors imply that a control strategy should be developed in order to achieve consistent and predictable vehicle behavior during braking (von Albrichsfeld and Karner) (Hancock and Assadian).

The ideal test vehicle for regen braking would possess one electric motor for each wheel, a variety of battery options, a power controller and the necessary ancillaries. However, such a vehicle project would have an intrinsic high level of packaging complexity, cost and time. To overcome these negative aspects, another concept was conceived, in which a hydraulic friction brake system is controlled to emulate electric motors.

1.3 Objectives

The objective of the Master Thesis is to design and develop a test vehicle with an Electro-Hydraulic Brake (EHB) system capable of emulating a regen braking system. The regen system is emulated in the sense that the friction brake wheel torque is equal to that produced by an electric machine.

The main use of the test vehicle is to analyze the limitations of additive regen braking, where additional electric motor brake torque is applied on top of the torque of the original (OEM) brake system. Additive regen braking allows the original brake system to be retained, saving production costs while giving fuel consumption improvements. Also, it facilitates the transition process to hybrid vehicles. The alternative to additive braking is brake blending, which smoothly changes the proportion of friction brake and regen torque. It requires the implementation of a brake-by-wire system in the production car. Since the test vehicle is primarily used for

development of additive regen braking, the original brake system is kept untouched. The test vehicle is then equipped with two brake systems; the OEM system and the EHB system.

The test vehicle should include software with the necessary vehicle subsystem models to translate requested wheel torque to required brake pressure output of the EHB. Generic models of electric driveline components such as electric motors, battery and power electronics should be developed to emulate an electric vehicle. Also, the software should have a modular architecture to aid development of new control models.

A use case analysis should to be conducted. The functionality of the proposed test vehicle might be useful for the development of other brake-based vehicle control functions, such as autonomous braking. Possible uses of the vehicle should be analyzed and their functional requirements taken into consideration when specifying the test vehicle.

A system safety analysis should be made to identify possible hazards and to implement the necessary features to handle these. A by-product of the safety analysis is a user guide booklet, giving instructions on precautions to take and procedures to use.

Testing is carried out to calibrate the software and evaluate the performance of the installed system. For calibration of the brake disc heat model, Hardware-In-the-Loop (HIL) testing is carried out. The function of the test vehicle is validated by measuring the precision and the response of the brake application.

1.4 Delimitations of work

All mechanical work is done by the Saab prototype and chassis workshops. All modeling work is done in Matlab/Simulink (not in lower level programming language such as C).

2 Use Cases

The possible use cases for the test vehicle are described to make sure it has the required functionality. The compilation of use cases was done with help from chassis & powertrain controls engineers from SAAB (Olsson, Klomp and Eklund). For all use cases, important software functions, performance requirements and required signals and sensors are identified.

2.1 Limitations of additive regen braking

The maximum brake torque of an electric motor varies with vehicle speed. Therefore, to produce constant deceleration for a constant brake demand for all vehicle velocities, the braking effort has to be smoothly blended between the electric motor and the friction brakes (von Albrichsfeld and Karner). The implementation of a brake-by-wire (BBW) system is a costly procedure. Also, it posts a number of new, mostly safety related, challenges (Hoseinnezhad and Bab-Hadiashar). An interesting topic is whether it is feasible to retain the standard mechanical-hydraulic brake system with added regen braking. This is called additive regen braking.

The pedal feel could be said to be the driver's perception of the correlation between the pedal input and the realized vehicle deceleration. Characteristics of the pedal feel include the brake controllability, progressiveness, effort and sponginess (de Arruda Pereira) (Rajesh, Badal and Pol). The pedal feel gives feedback on brake performance (Day, Ho and Hussain), influences the perceived quality of the brake system and is important for the driver's confidence in the system (Pascali, Ricci and Caviasso). As the amount of additive regen increases, the regulation required and the effects of electric driveline failure increases as well. The problem is to determine how much additive regen braking can be done before the driver perceives the additive braking as unpredictable and unsafe.

Figure 1 displays a suggested functional model for this use case. This can be said to be the flow of information through the control system of the test vehicle. The starting point is the input parameters, which are then used by function blocks, representing a strategy or a modeled subsystem. The output is the requested EHB brake torque values at the wheel of all four corners of the car.

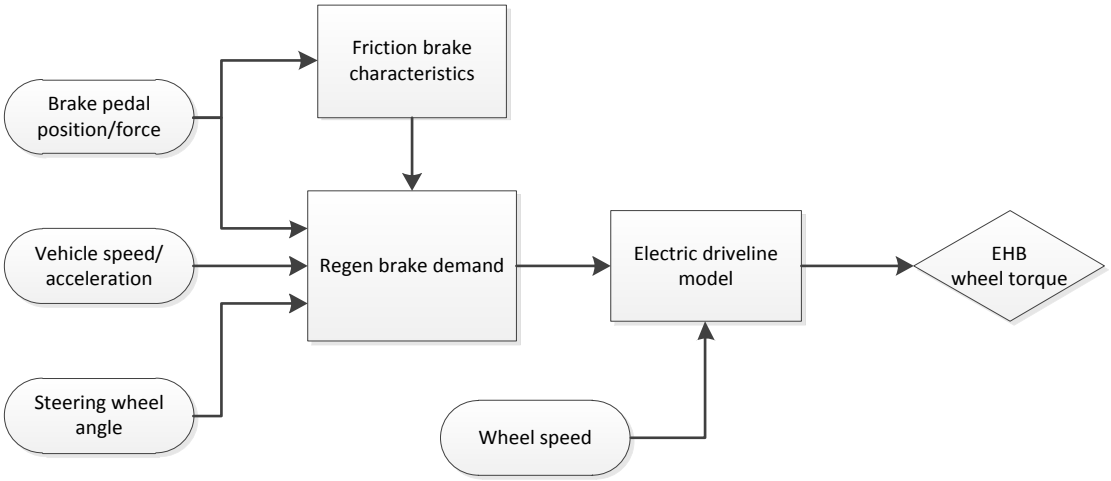

Figure 1. Functional model of additive regen braking use case

The regen brake demand function determines how much additive braking that should be done. This function could work in any way determined by the test engineer. However, useful inputs to this function include brake pedal displacement, brake master cylinder pressure and vehicle speed. Also, it is preferable to have knowledge about some characteristics of the original brake system, for instance the brake pedal travel vs. brake pressure curve. The electric driveline model then calculates the maximum achievable torque from the motor, and limits the requested regen torque values if necessary. The driveline model could be a simple torque vs. speed curve. However, the peak torque output of an electric machine is time-dependant due to heat buildup in the windings. A heat model of the electric motor is needed to fully capture this characteristic, which is relevant for short and intensive braking scenarios.

2.2 Influence of regen braking on handling and stability

In vehicle dynamics, handling is connected to how well the car follows the intended path of the driver, which is a relative measure. Stability describes how well the vehicle body slip angle response is controlled as a result from an external force (Milliken and Milliken) (Blundell and Harty). Aside from keeping the car from spinning out of control, the car should also be kept from rolling over (Hopkins, Taheri and Ahmadian).

The front to rear brake bias highly affects handling and stability. Shifting the brake bias rearwards translates into the rear wheels locking earlier, which in turn alters the handling and may cause vehicle instability. When a brake source is added, as when regen braking is performed, the brake bias is affected. If regen braking is done at the rear axle, the braking torque provided by the motor must be controlled in order to not give unwanted rearwards brake bias. A simple strategy to maintain vehicle stability with regen braking at the rear would be to ramp out electric torque generation once the longitudinal slip of a rear tire exceeds a certain threshold value (Hancock and Assadian), or when the Anti-lock Braking System (ABS) or Electronic Stability Control (ESC) is activated.

A functional model for this use case would be very similar to that in Figure 1. Interesting parameters to be fed into to the brake demand function include longitudinal tire slip, vehicle acceleration and yaw rate. Also, the activation of the ABS and ESC units should be monitored.

Another parameter that would be useful for this use case is the road friction coefficient. In (Shim and Margolis), great improvements in vehicle stability control were shown when the road surface friction was known. In (Andersson, Bruzelius and Callesgren), an implementation of a road friction estimation system was done. Considering this, the test vehicle should be able to incorporate signals from instruments used to measure the road friction, for instance force transducers and optical sensors.

2.3 Friction and regen brake transitions

Braking transitions include every case when the standard friction brakes or the regen braking are put on or off. Needless to say, the time response and the driver's perception of the change in brake torque are of main interest. At the event of a panic braking, the regenerative braking is ramped out to zero since it may cause vehicle instability. It is vital that the friction brake modulator is quick enough to cover the requested braking effort during the regen ramp out. Otherwise, the driver might sense the transition as a sudden lack of brakes. If the regen brakes are off completely before the friction brakes are applied, the driver might even get the feeling of acceleration. The seriousness of the matter can be exemplified by Toyota, which 2010 was faced with having to recall their Prius (BBC news). Customers complained about the car feeling unsecure during braking.

For a brake transition strategy function, the value and rate of change of brake pedal displacement can be used to recognize panic braking. Other interesting parameters to observe are wheel slip and vehicle longitudinal acceleration. The brake pressures of the standard brake system could be used to calculate the buildup of friction brake force.

2.4 Coast regen braking

Coast regen is the application of regen braking during zero driver braking and throttle input; during coasting. The amount of regen braking performed is relatively small. It is possible to compare the scenario as being similar to increasing the amount of internal combustion engine braking. If the throttle travel goes from point A to point B, the point of zero engine torque can be moved slightly from point A towards point B. Letting off the throttle pedal completely would then result in a negative propulsion torque request. The main interest in the coast regen use case is to evaluate the driver's perception of this increased engine braking. The limit of coast regen is set by what the driver perceives as comfortable. This use case might be investigated together with the limitations of additive braking use case. Since the maximum amount of recuperation is lower for additive regen braking than for a blended braking system, more coast regen can be implemented to recuperate useful amounts of energy.

An important input for a coast regen strategy function is the throttle pedal (accelerator) position. Other vehicle states, such as the vehicle speed and engine torque might be desired.

2.5 Other applications

Essentially, the EHB system of the test vehicle delivers wheel torque according to the implemented software. This general function may be useful for testing of various vehicle systems, even those unrelated to regen braking.

The test vehicle can be used for development of active safety systems. This could be crash mitigation/prevention or avoidance maneuvers. Crash mitigation deals with sensing a possible hazard and decreasing the severity of the situation by decelerating the car. Avoidance maneuvers use the brakes to steer the car out of harm's way.

Torque vectoring distributes the propulsion torque between the four wheels to aid maneuverability. In the test vehicle, torque vectoring can be achieved by using the friction brakes to brake one of the front wheels, while adding propulsive torque to maintain the vehicle speed. This approach is lighter and cheaper compared to complex electro-mechanical devices and adds functionality to already existing components.

Many vehicle systems that use the brakes for functionality can be developed using the test car. The control system of the test vehicle should have interfaces to implement any required sensory information.

3 Electric Vehicle Subsystems

The basis of the test vehicle's EHB control system functions requires knowledge of friction brakes theory. Also, the regenerative braking application of the vehicle requires basic theory on electric motors, batteries, and power converters.

3.1 Friction brakes

Equation 3.1 shows the relationship between brake pressure p, caliper piston area A, brake torque T, the number of pistons n, the number of brake pads m, pad/disc friction coefficient μ, and average pad radius r. The average pad radius is measured from the center of the disc to where the total friction force from the pad is applied.

$$T = Fr = npA(m\mu)r$$

$$p = \frac{T}{mnA\mu r} \qquad \text{Equation 3.1}$$

All the variables needed to calculate brake pressure are known. However, the pad/disc friction coefficient varies depending on the brake disc temperature. An example curve is shown in Figure 2 (IBT Power Ltd.).

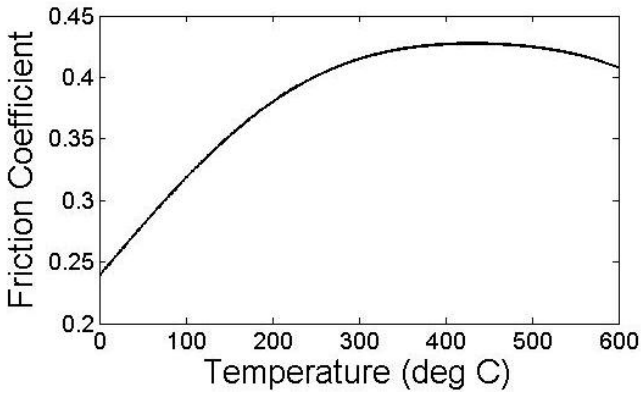

Figure 2. Friction coefficient vs. temperature

To get the brake disc temperature, a brake system temperature model was created in Simulink instead of using temperature sensors due to the price, reliability, and dust/debris sensitivity of such sensors. The next chapter describes the equations used for this model.

3.1.1 Brake system thermodynamics

Friction brakes work by converting kinetic energy into heat. This rate of heat generated $\dot{Q}$ can be expressed in terms of torque T and angular velocity ω.

$$\dot{Q} = T\omega \qquad \text{Equation 3.2}$$

The heat Q is generated in a third body between the brake disc and brake pad, which is formed by detached particles (Talati and Jalalifar). This third body spreads the heat onto the brake pad and brake disc through imperfect contact. The amount of heat transferred through imperfect contact is proportional to an imperfect contact coefficient which may not be the same for the pad and the disc. Both the pad and the

disc have masses that absorb the heat energy. The amount of heat energy absorbed is dictated by the definition of specific heat, Equation 3.3, where m is the mass, c is the specific heat, and ΔT is the difference in temperature between two instances.

$$Q = mc\Delta T \qquad \text{Equation 3.3}$$

Once the heat is transferred to the brake disc and brake pad contact area, it will conduct into the rest of the brake disc. The thermal conduction behavior is described by Fourier's Law, Equation 3.4, which assumes heat is transferred along an axis with only one degree of freedom. In this equation, Q is heat energy, k is the thermal conductivity, A is the cross sectional area, x is the distance in which the heat has travelled, and ΔT is the temperature difference across x.

$$Q = \frac{kA}{x}\Delta T \qquad \text{Equation 3.4}$$

Equation 3.4 can be used to derive Equation 3.5, the formula for conduction in the radial direction, as shown in Figure 3.

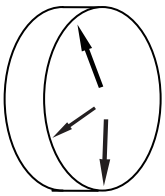

Figure 3. Thermal conductivity radial direction

$$Q = \frac{2\pi kt}{\ln r_o/r_i}\Delta T \qquad \text{Equation 3.5}$$

In Equation 3.5, Q is heat energy, k is the thermal conductivity, t is the thickness of the material, r_o is the outer radius, r_i is the inner radius, and ΔT is the temperature difference across r_o and r_i.

Using both Equations 3.4 and 3.5, the brake disc and brake pad can be broken down into many separate elements to allow a better simulation of the temperature gradient of the different regions of the brake disc. It should be noted that both the specific heat and the thermal conductivity of brake pads are not constants but rather dependent on temperature.

After the heat has traveled to the brake disc and brake pad, the only way for it to escape to the surrounding air is through convection. Convection behavior can be expressed by Newton's Law of Cooling, Equation 3.6, where Q is heat energy, h is the convection coefficient, A is the surface area, and ΔT is the difference in temperature between the surface and the surrounding air.

$$Q = hA\Delta T \qquad \text{Equation 3.6}$$

The main unknown in this equation is the convection coefficient, which is highly dependent on the object's geometry and airspeed. There is no general theoretical model for calculating the convection coefficient in terms of speed (Elert). The following equation is used along with experimental calibration to obtain a convection model (Elert).

$$h = X + Y * \sqrt{v} - v \qquad \text{Equation 3.7}$$

Since the brake disc has a very complex geometry, with air vents sandwiched between two thick iron plates, the convection coefficient may not be the same for all these surfaces. Dividing the brake disc into various elements helps cope with this challenge. This is further explained in Chapter 4.3.

3.2 Electric machines

The general concept of how electrical machines generate force is through the use of magnetic flux and electrical current. Picture an apparatus where a wire floats in a perfectly linear magnetic field, with gravity and air resistance being negligible (Figure 4*Figure 4*). It turns out that if a current is applied across the wire, a force is generated on the wire with the direction of it being perpendicular to the field and the wire.

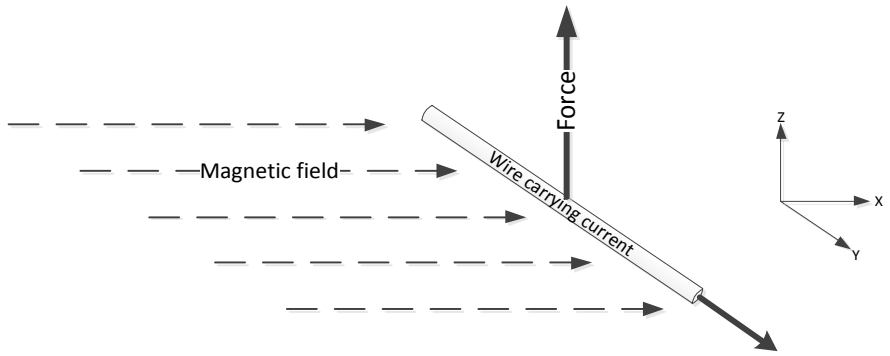

Figure 4. Force produced by a wire carrying current in a magnetic field

The relationship between the force on the wire F, flux density in the magnetic field B, the current in the wire I, and the length of the wire l is shown by Equation 3.8, also known as Lorentz force (Hughes).

$$F = BIl \qquad \text{Equation 3.8}$$

With a force now applied, the wire will have a velocity. When a wire "cuts" through the magnetic field as shown in Figure 5, an e.m.f. will be induced in the wire. The induced voltage will always try to create a current in the direction that would decelerate it. Faraday's Law, Equation 3.9, shows that the amount of e.m.f. E depends on the flux density B, length of the wire l, and the velocity v.

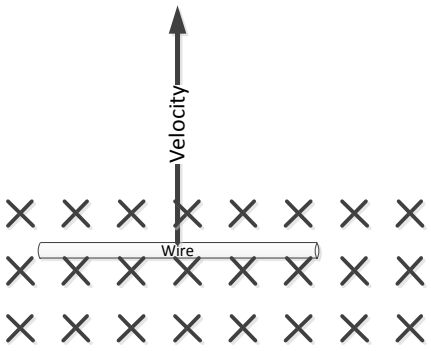

Figure 5. A wire cutting through a magnetic field

$$E = Blv \qquad \text{Equation 3.9}$$

3.2.1 Equivalent circuit

The wire from Figures 4 and 5 above is put into an equivalent circuit with a supply voltage V, wire resistance R, and the induced e.m.f. E in Figure 6 below. The physical wire is represented by its resistance, as well as the e.m.f. across it when it cuts through the magnetic field.

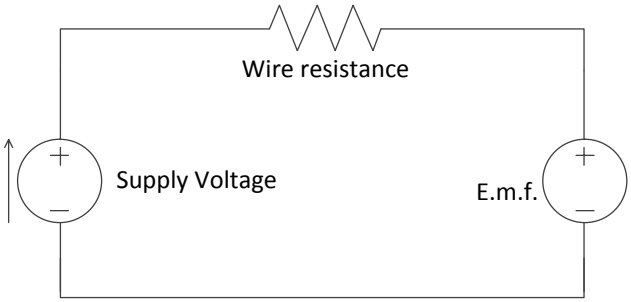

Figure 6. Equivalent circuit of wire in a magnetic field

In this circuit diagram, the supply voltage pushes current clockwise, while the e.m.f. drives current counter clockwise. The circuit is described below using Kirchhoff's voltage law.

$$V = IR + E \qquad \text{Equation 3.10}$$

This is a very important equation because it explains almost all the phenomena involved with electrical motors. If solved for the current, the result is shown below.

$$I = \frac{V-E}{R} \qquad \text{Equation 3.11}$$

Recall that if the wire is at rest, there would be no e.m.f. voltage. Therefore a current will pass through the wire resistance with the amount being $I = V/R$. As the wire speeds up, the e.m.f. will increase based on Equation 3.9, and the current through the wire will decrease. This decrease in current will lead to a decrease in force, which also means a decrease in acceleration. So as speed increases, acceleration will be lower and lower until an equilibrium is reached where $V = E$. There would be no acceleration and the top speed is reached.

Suppose that the air resistance drag on the wire is not negligible. In that case, in the situation above, the top speed equilibrium would not be when $V = E$, because there would be no force on the wire to oppose the drag force. Therefore, some current is needed in the wire and the amount of current can be calculated using Equation 3.12.

$$I = \frac{F_{drag}}{Bl} \qquad \text{Equation 3.12}$$

After substituting this into Equation 3.10, the new equilibrium equation is derived.

$$V = IR + E = \frac{F_{drag}}{Bl} * R + E \qquad \text{Equation 3.13}$$

In all the situations analyzed, the supply voltage was always greater than or equal to the e.m.f. voltage. Consider another situation that initiates with $E > V$. In the physical sense, this means that the wire is traveling faster than the top speed that is achievable with the instantaneous conditions such as supply voltage, wire length, flux density, etc. This situation can happen due to external forces accelerating the wire or the supply voltage being lowered. Previously, an expression for current was derived from

the equivalent circuit equation, Equation 3.11. If $E > V$, $I < 0$. This means that the current has reversed direction. There are two significances to this. Firstly, a current going in the opposite direction will yield a force in the opposite direction. Therefore, the wire will slow down until it reaches the equilibrium defined by Equation 3.12. Second, the current will start going into the supply voltage, charging it instead of discharging it. This is the phenomenon that is used for regenerative braking.

It is important to note that if $V < 0$ and $E > 0$, I will be negative, but since the voltage terminals have been switched as well, I will be in the same direction as the voltage. This means that the motor will be braking, but not regenerating energy. Therefore for maximum regenerative braking, $V = 0$.

3.2.2 Field weakening

If the current and resistance is kept constant in the equivalent circuit equation shown in Equation 3.10, then as voltage increases, induced e.m.f. increases. According to Equation 3.9, E and velocity v has a direct relationship. This means that the supply voltage controls the top speed of the wire, and as previously explained, current affects the force. However, the e.m.f does not only depend on v, but also on the length of the wire l, and the flux density B. While the wire length is difficult to manipulate in the physical world, the flux density is not. In fact in electrical motors, lowering the flux density, or field weakening, is used often to lower the e.m.f. generated for a given speed. This allows for a higher top speed without requiring a higher supply voltage. However, since $F = BIl$, field weakening also decreases the magnitude of force applied onto the wire (Hughes).

3.2.3 Application of electric-magnetic theories to a simple brushed DC motor

An electrical machine, regardless of type, tries to exploit the previously explained theories into a rotational machine. The math and science is exactly the same as the previous example of a wire in a magnetic field, with a couple new variables that are specific to motors.

In electric motors, instead of force, there is torque. Rotational velocity is used instead of linear velocity. $F = BIl$ is replaced by Equation 3.14, where k_t is the torque constant and T is the torque.

$$T = k_t I \qquad \text{Equation 3.14}$$

The equation for the induced e.m.f. is also different with a new variable, e.m.f. constant or k_e being introduced.

$$E = k_e \omega \qquad \text{Equation 3.15}$$

These constants are characteristics of the motor at hand. Note that in both equations, since they are derived from the primitive Equation 3.8 and 3.9, the constants k_t and k_e are directly proportional to flux density B. Therefore, the idea of field weakening will change the torque and e.m.f. constant of the motor. Figure 7 below is a torque vs. speed curve of a generic motor.

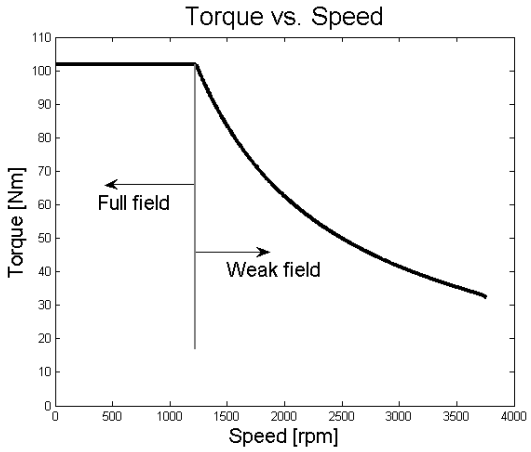

Figure 7. Torque curve showing the full field and the effects of field weakening

It is pragmatic to know that in SI units, $k_t = k_e = k$. This can be proven by their units since $k_t = Nm/A$ and $k_e = Vs/rad$.

$$\frac{Nm}{A} = \frac{J}{A} = \frac{Ws}{A} = \frac{VAs}{A} = \frac{Vs}{rad}$$

Knowing this, one can trade torque for speed by choosing a motor with a lower torque and e.m.f. constant, and vice versa. In order to achieve high torque and high speeds, a high supply voltage is required.

The relationship between supply voltage, induced e.m.f., and current is still the same as it was for the wire in a magnetic field example. The only difference is that there are now new values for solving E and T. Using the new expressions for E and T, a new equivalent circuit equation can be formulated.

$$V = E + IR = k_e\omega + \frac{T}{k_t}R \qquad \text{Equation 3.16}$$

3.2.4 Mechanical workings of an electric machine

Figure 8 below shows a cross section view of a simplified brushed DC motor. To illustrate the components clearly, there are only 8 coils, in the rotor, which is much less than the amount in real rotors. Each coil is two connected wires on opposite ends of the rotor, so in reality it is one long wire with a downward flowing magnetic field. The wires on the top will produce a force towards the left, and the wires on the bottom will produce a force towards the right. This results in a counter-clockwise torque.

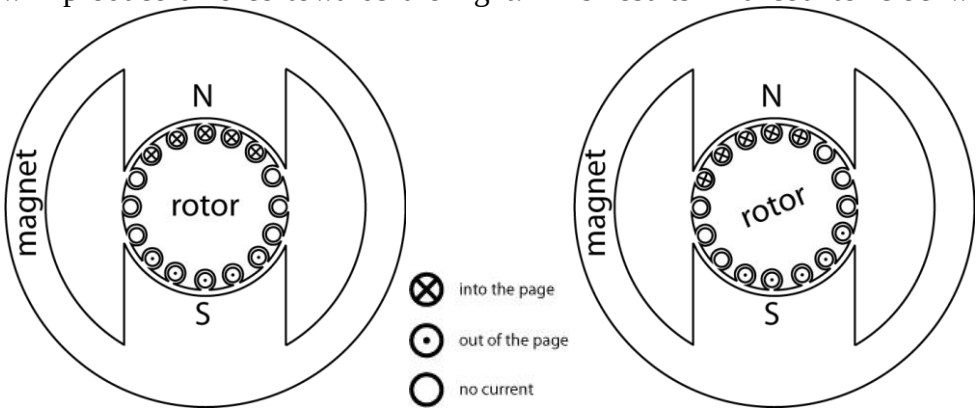

Figure 8. (left) Brushed DC motor, (right) Counter-clockwise rotation of the rotor

With the torque on the rotor, it will start spinning counter-clockwise. If the coils are continued to be connected to the supply in the same fashion, later on the motor will look like Figure 9 (left). Brushes and commutators are components that reverse the coils' contacts with the supply to switch its current direction. Figure 10 (right) below shows a single coil of the previous motor to clarify the function of the brushes and commutators.

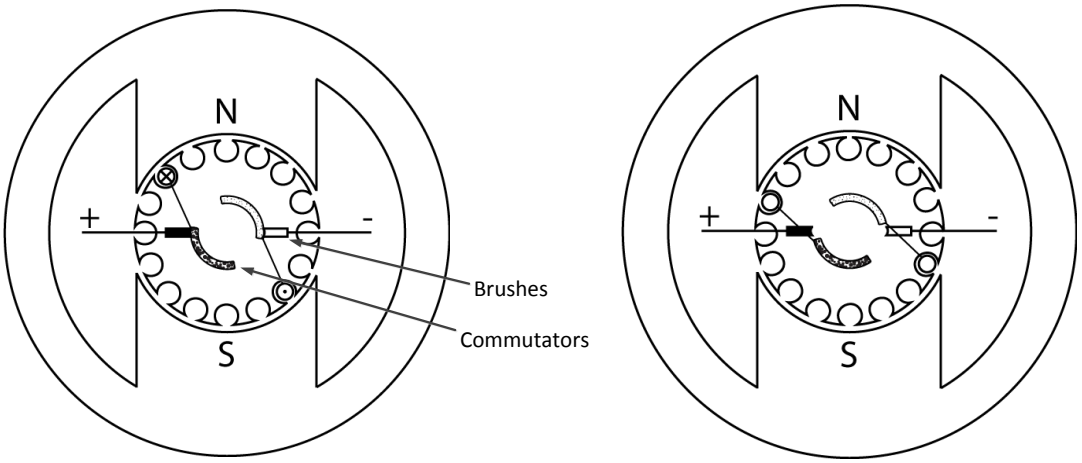

Figure 9. (left) Brushes and commutators for a single coil, (right) commutators disconnected from the brushes, resulting in no current in the coils

The coils and commutators all rotate together with the rotor. The brushes, however, are stationary and are connected to the supply voltage. It is important to note that the brushes do not contact just one coil, but all the coils in the machine. While there is a pair of commutators for each coil, there are only two brushes for the machine. Figure 10 below shows what it would look like with the rest of the coils and commutators installed.

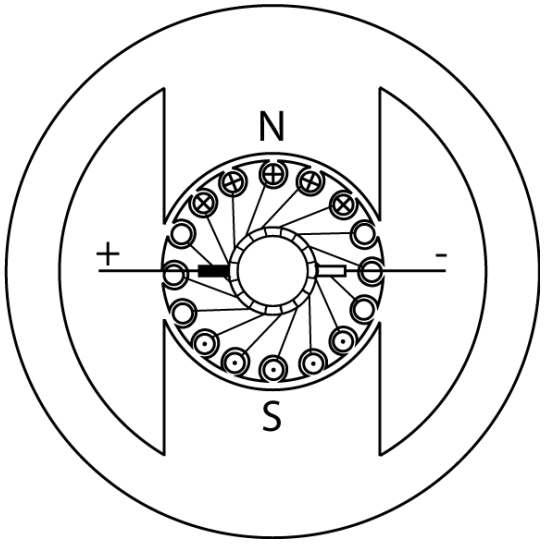

Figure 10. Full motor diagram with all coils and commutators

3.3 Batteries

Batteries provide current through a cathode and an anode, which is the positive and negative end of the battery, respectively. By nature, electrons at the anode are attracted to the cathode. However, an electrolyte in the battery separates these two ends of the battery, and the electrons have to find another route to the cathode. This is why, when the battery is connected to a load, current passes through, since it is the only way for electrons to reach the cathode.

There are various types of batteries used for vehicles. Lead-acid is usually used for normal car batteries due to their longevity, but are heavy relative to their capacity. For hybrid vehicles, Lithium-ion batteries are used instead. Some electric race motorcycles use super capacitors due to their high discharge rates and low weight despite their low energy capacity. These characteristics of batteries are explained in more detail below.

3.3.1 State of charge

The state of charge (SOC) is the amount of charge in the battery expressed as a percentage of the maximum amount of charge. It has a great effect on the maximum voltage of the battery. Figure 11 below shows the typical maximum voltage for a range of state of charge (IBT Power Ltd.).

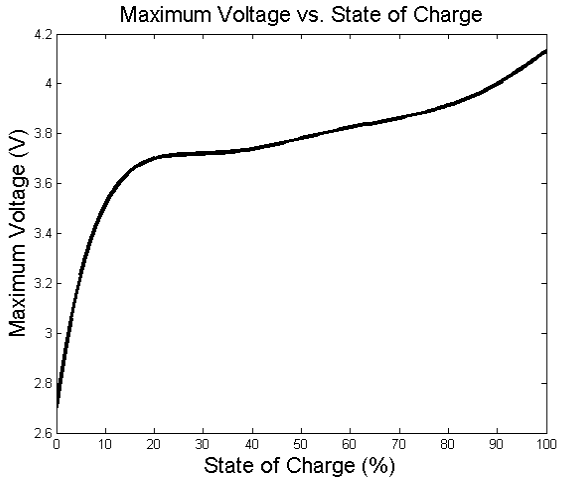

Figure 11. Typical maximum voltage vs. SOC curve

It is apparent that in the state of charges where the battery is almost completely discharged, the maximum voltage decreases exponentially. This is one of the reasons why electronic devices do not completely discharge the battery. The other reason has to do with battery health, which will be explained in the next section.

3.3.2 Battery health

During operation, batteries are discharged and recharged. Repeated cycles of discharging and charging will age the battery. With age comes poorer battery capacity. The maximum amount of charge that the battery can hold will decrease. Typically, batteries have specifications on the maximum number of cycles before the battery can be considered flat. The definition of a cycle is generally a discharge of a certain amount of state of charge and a recharge to its original value. The amount

discharged depends on the manufacturer, and can be anything from 30% to 80%. This is the reason why car manufacturers prefer to keep their batteries between a certain percentages of charge in order to prolong battery life, usually 40% to 60% (Hoffman). The change in maximum capacity versus the number of cycles is generally very linear, see Figure 12.

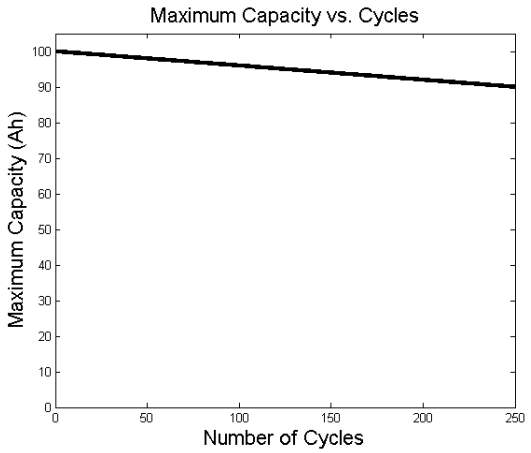

Figure 12. Typical state of charge vs. cycles graph

This type of capacity vs. cycles curve is usually experimentally obtained at a certain charge and discharge rate. The faster the battery is being charged or discharged, the worse it is for the battery health and the lower number of cycles it will sustain before it is flat.

3.3.3 Charge and discharge rates

Charge rate and discharge rate is how quickly charge goes into or out of the battery. This is also known as current, but when describing batteries, often Ampere is not the unit of measurement for charge and discharge rates. The dimensionless unit of C-rate and E-rate is used for charge and discharge rate correspondingly. These units measure current by the amount of current to charge or discharge the entire battery capacity in 1 hour. A charge rate of 1C means the amount of current to fully charge the battery from 0 Ampere-hours. A discharge rate of 2C means twice the amount of current to fully discharge the battery from full. Note that this unit of measurement depends on the battery capacity. Therefore, to meet the current needs for the motor, the battery capacity as well as the charge and discharge rates needs to be examined.

3.4 Power controller (Inverter)

The power controller is usually the same unit used to take in the supply voltage and output to the motor the amount of voltage desired by the user. The most primitive way to do this is to have a variable resistor in the circuit to control the motor by adjusting the resistance. The resistance then takes up some of the supply voltage, and the left over voltage is applied to the motor.

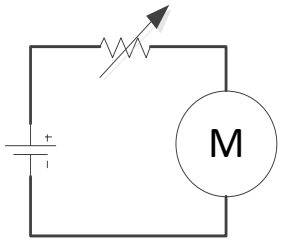

Figure 13. Primitive voltage controller

This type of control works fine, but when efficiency is taken into account, the resistor is taking up a fraction of the voltage and converting it to heat. If the motor is controlled to not move, then all of the battery's energy is wasted in the resistor, resulting in an efficiency of zero.

The modern way to control voltage is through the use of electronic switches. In Figure 14, the variable resistor from the previous example is replaced by a mechanical switch.

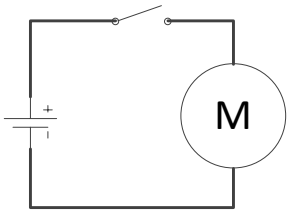

Figure 14. Motor voltage control through the use of a switch

If the switch is open, then the motor would receive no voltage. If it was closed, then it would receive 100% of the battery's voltage. If the switch repeatedly opened and closed, then the resulting voltage vs. time graph could look like Figure 15*Figure 15*.

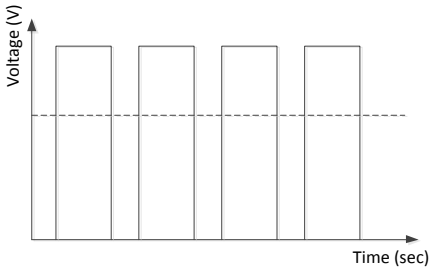

Figure 15. Switching strategy of motor control with average voltage

It happens that when done quickly enough, the average voltage, shown by the dotted line, is smooth enough for an electric motor. To change the average voltage, the width of each pulse or the repetition of each pulse can be varied. With the mechanical switch, assuming no losses in the switch, there is 100% efficiency; no energy is wasted to reproduce the same control as the variable resistor. In reality, this type of switching is done with electronic switches such as a transistor to obtain high switching frequencies and reliability. Transistors do require a small current in order to turn the switch 'on', therefore sacrificing some of the supply voltage but still maintaining a very high overall efficiency of the system.

It is not very important in this project to model and understand the complexities of the power converter, since they mostly deal with flexibility and efficiency of the electronics. In this thesis, the power converter was modeled in a very simple way, with the power drawn out of the battery being a little higher than the power required by the motor due to some user defined constant efficiency value. In practice, very often the motor characteristics are modeled along with the controller and power converters required to operate the motor.

4 Regenerative Braking Emulation Modeling

For all purposes of the test vehicle, the EHB unit requires CAN messages to be sent from the software in order to apply pressure to the brakes. Overall, the software includes sensor data processing functions, the test function and the translation from requested torque to EHB pressure. To translate torque to pressure, a model of the brake system is required. For the purpose of regen braking simulation, virtual electric driveline components are implemented.

4.1 Control system architecture

It is desirable to make the test vehicle software versatile and easy to modify. To make sure this is the case, the layout of the control system is analyzed.

The functional architecture can be said to be the overall organization of all actuators, sensors and functionality. A layered or hierarchical functional architecture greatly enhances the extensibility and reconfigurability of the system (Coelingh, Chaumette and Andersson). Importantly, there should be no interaction between the modules at a certain level (except for the top layer) and all driver inputs should pass through the bottom layer.

Figure 16 shows the functional architecture of the EHB system.

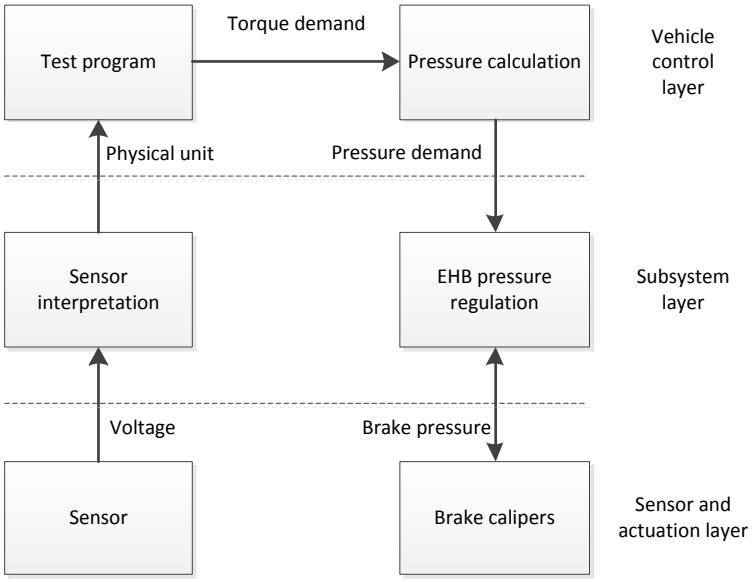

Figure 16. Functional architecture of the control system

At the top level, the test program is quite simply the function that is to be tested. Often most, some input data is required that might have to be transformed from sensor voltage to a physical unit. The number and types of sensors used might differ between use cases. The output of the test program is the torque request for all four wheels. The other top-level block consists of a brake model, which calculates the required brake line pressures to accomplish the desired brake torques. The rest of the chain is hardware specific and shouldn't necessarily be altered for different use cases. The EHB pressure regulation depicts the internal regulation of brake pressure in the EHB unit.

4.2 Overview of modeled subsystems

All modeled vehicle subsystems are described using flowcharts due to their complexity. These describe the flow of information and the functions used. Each flowchart module is detailed according to Table *Table* .

Table 1. Flow chart block shapes and their descriptions

Shape	Description
	Inputs
	Outputs
	Processes, calculations, sub-models
	Pre-defined parameters

For a use case with regen braking emulation, the functionality of the software is described by Figure 17.

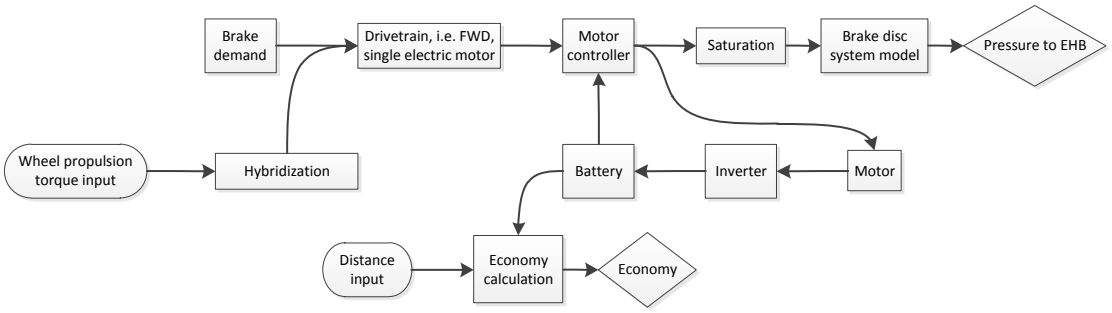

Figure 17. Software layout of the test vehicle emulating regen braking

Three distinctive functions can be identified. The brake demand module is where the test vehicle user implements the regen brake strategy. Naturally, this function is different from use case to use case, but it is consistent in the way that the output is always the desired brake torque for all four wheels. Another distinctive function could be said to be the electric drivetrain modules. Basically, this string of smaller subsystems saturates the desired brake torque to the level achievable by the electric drivetrain. The last distinctive function is the brake disc model which calculates the required brake pressure.

It should be noted that not only the braking mode of the electric drivetrain is taken into account. The requested propulsion torque is monitored in the test vehicle and fed into the drivetrain models. By saying that the electric motor should provide a certain amount of drive torque, the virtual motor will function in both propulsion and generator mode. This means that the state of charge of the batteries will both decrease and increase during vehicle operation. Of course, the actual propulsion felt by the driver is from the combustion engine.

For software debugging of the test program, a vehicle simulation module is implemented. This is described in Chapter 6.1.

4.3 Brake disc system

The brake disc system mainly translates the desired EHB brake torque to pressure using Equation 3.1. Since the friction coefficient is function of temperature, the calculated brake torque of the standard (OEM) brake system and wheel speed inputs are required to calculate the heat generated. These inputs can differ for each wheel of the car and therefore four separate brake disc models are used to calculate the pressure required.

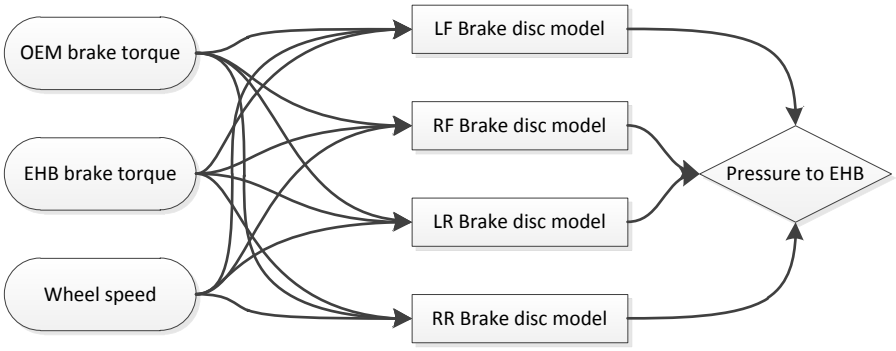

Figure 18. Brake disc model layout.

4.3.1 Brake disc models

To calculate the EHB pressure from the brake torque desired, Equation 3.1 is used. The temperature model calculates the brake disc temperature using Equations 3.2 to 3.7. Either the brake disc or brake pad temperature can be used to calculate the temperature dependent friction coefficient. The friction coefficient vs. temperature curve is determined during testing of the final vehicle.

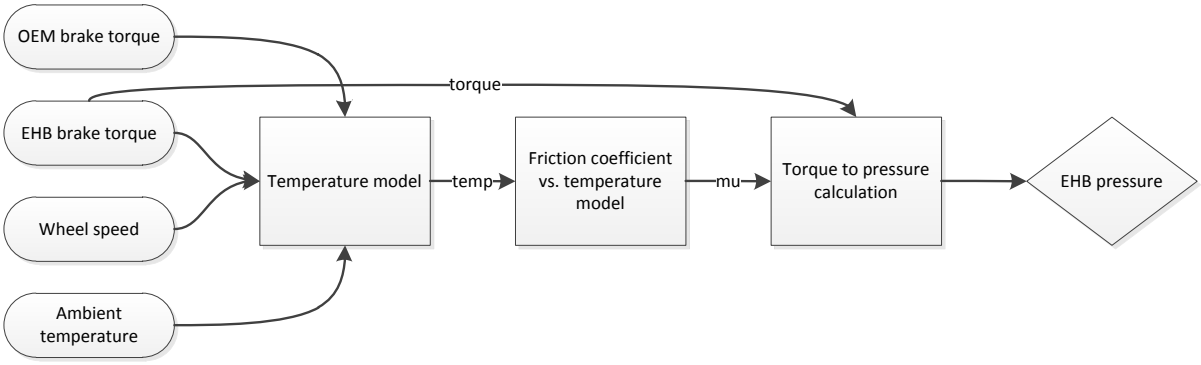

Figure 19. Brake disc functional model

Three temperature models were developed to calculate the disc temperature. The simplest model considers the entire brake disc as a lumped mass with the same temperature, convection, and heat input properties (Figure 20 left). The other two models divide the brake disc into four main elements. One of the models divided the disc in a pie pattern (Figure 20 center). This allows modeling of the recently heated part of the brake disc separately from the rest of the disc. The model on the right divided the disc in a radial fashion, which allows the outer parts of the brake disc to

heat up at a different rate than the inner parts (Figure 20 right). This flexibility was inspired from the observation that there is more brake pad material in contact with the outer radii of the brake disc than the inner radii.

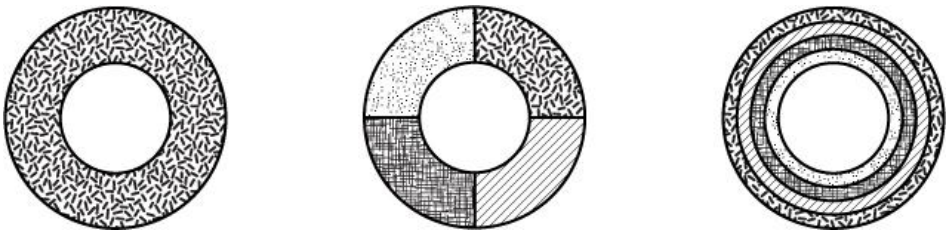

Figure 20. The three different brake disc models from left to right: the lumped mass, the pie pattern, and the radial pattern model.

4.3.1.1 Lumped mass

This model considers the heat of the brake disc to be uniform throughout. The brake heat provided by the OEM and EHB brakes heats up the pad and the disc through an imperfect contact. A portion of the heat goes to heating up the surrounding air. Figure 21 shows the functionality of the lumped mass temperature model.

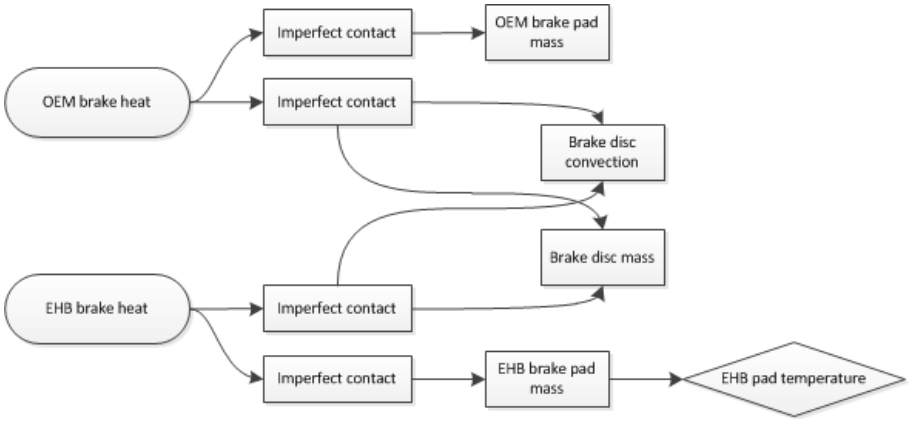

Figure 21. Lumped mass temperature model

4.3.1.2 Pie pattern

In the pie pattern temperature model, the brake disc is divided into four parts. The objective is to model the fact that heat is not applied to the entire brake disc at the same time, but only at specific parts of it. The idea was that the area of the brake disc that was recently heated would have a higher temperature than the part that will be heated next. Therefore, heat is applied only to one element at a time with each element bearing ¼ of the total mass and ¼ of the total convection.

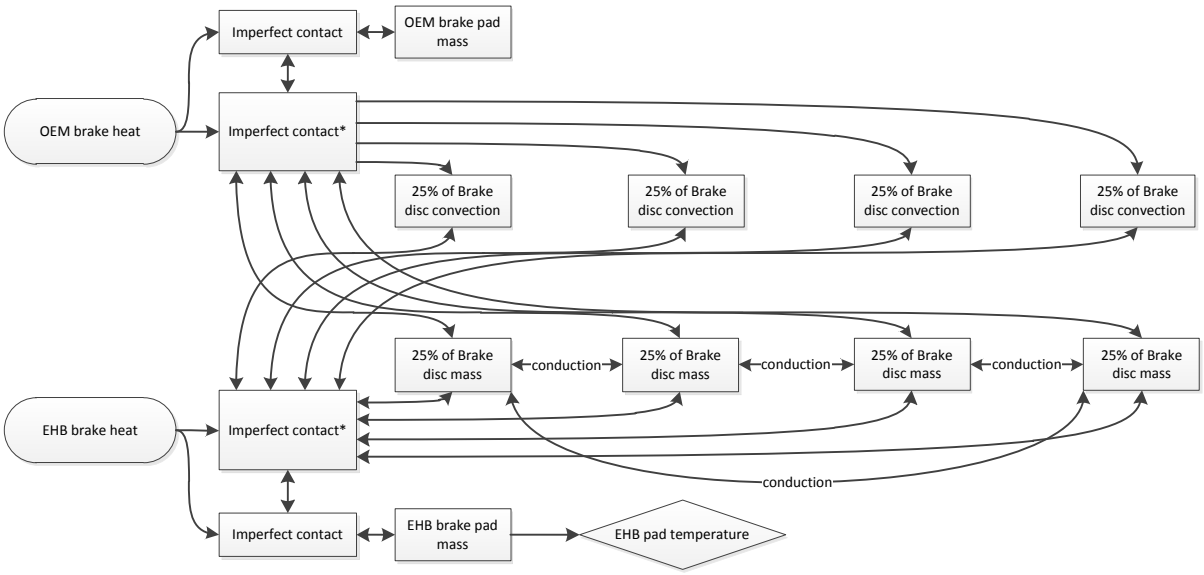

*Figure 22. Pie pattern temperature model. *Heat is output only to one convection block and one brake disc mass at any instant*

Figure 22 above shows the layout of the pie pattern temperature model. An algorithm for the heat applied is developed so that heat is injected to only one element at a time. Also, the two-way arrows depict the heat movement going in both directions. For instance, heat can travel from the brake disc to the brake pad or the other way around, depending on the temperatures of both.

When testing the model, it was soon realized that this temperature model did not differ much from the lumped mass model. The temperature readings on the brake disc elements were within 1 degree of each other. The difference between the average brake disc temperatures of the two models were within 2 degrees of each other, which yields negligible effect on the friction coefficient model. This most likely means that in most cases, the brake disc is spinning quickly enough to distribute the heat very evenly on all four elements.

4.3.1.3 Radial pattern

The radial pattern divides the brake disc into concentric circles. Like the pie pattern model, there are four elements. Unlike the pie pattern model, the spinning of the brake disc is not simulated, and therefore, for two given brake heats, the heat is supplied to each element continuously.

However, this model takes into account two phenomena: the different brake pad sizes between the two brake systems, and secondly, the different amount of pad surface being in contact with the brake disc at different radii. For the first point, the OEM brake calipers cover almost the entire useable radius of the brake disc, whereas the EHB brake calipers cover a fraction of the useable radius of the brake disc. This will result in hotter brake disc temperatures on the disc surfaces where both brake pads come into contact with. Secondly, brake pads are shaped in a way where there is more contact surface area on the outer radius than the inner radius (Figure 23). This results in higher disc temperatures on the outer radii of the brake disc. Higher disc temperatures will yield higher brake pad temperatures due to heat transfer between the two units.

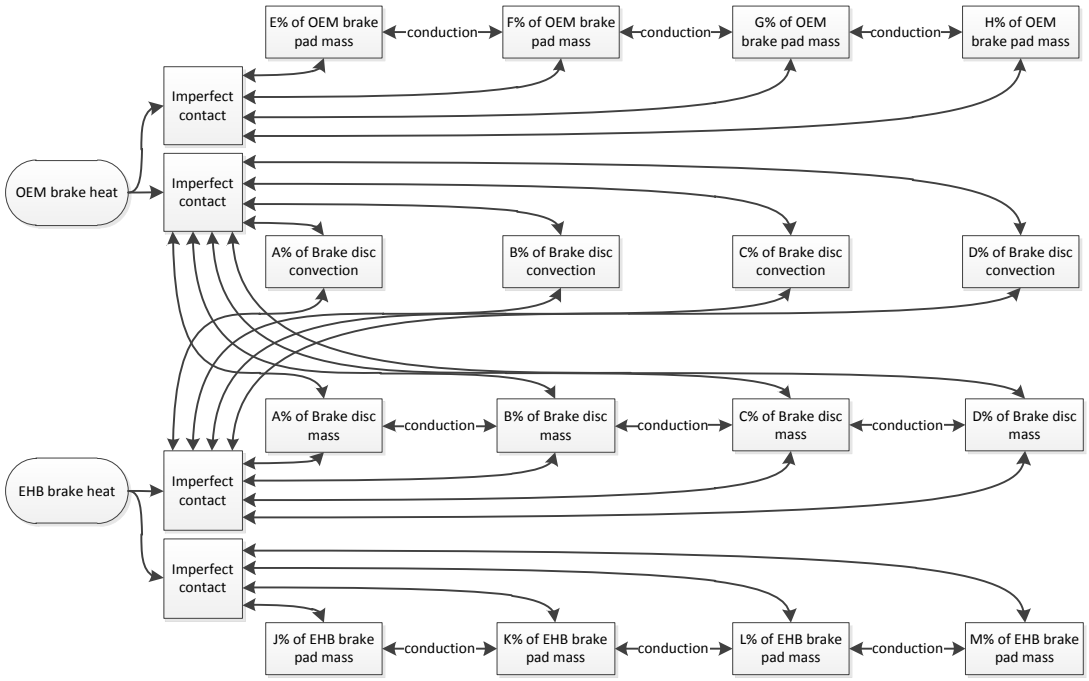

Figure 23. Radial pattern temperature model functional diagram

This model showed great differences in temperature when compared to the lumped mass and the pie patterned model using the same disc and pad properties. It also showed a great temperature gradient throughout the radius of the brake disc. Due to higher flexibility, and the lack of time to calibrate all three types of temperature models, the radial pattern temperature model was adjusted to match experimental results. During experimentation, it was realized that the heat on the surface of the brake disc can take some time to conduct into the brake disc vents. In other words, there needs to be more elements dividing the surface of the brake disc and the vents.

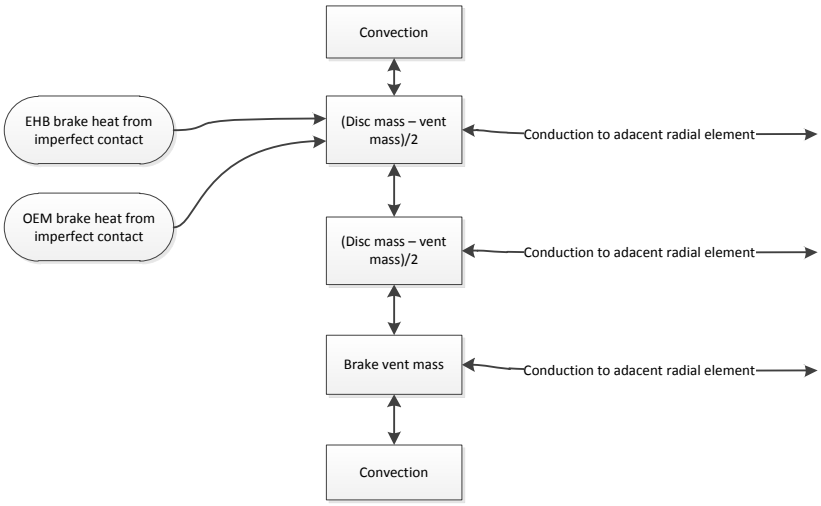

Figure 24. Each X% of brake disc mass was further divided into three elements.

This further division allowed more adjustability with the convection coefficient.

4.4 Brake demand

The brake demand module is where the test user implements the functions to be tested. Therefore, the input parameters are largely determined by the user. The output should however always be the desired wheel torque for each corner of the car.

One function is included in this module. In the use case analysis, it was concluded that some information of the standard brake system might be useful for development of the tested functions. Therefore, the brake demand model takes in the front and rear OEM brake pressures and outputs the brake torque of the OEM brake system. The torque is calculated using Equation 3.1, where the friction coefficient is an input from the brake disc system model.

The overall structure of the brake demand block is shown in Figure 25. Note that the OEM brake torque calculation is used in the brake heat model and should be retained unless constant friction is used.

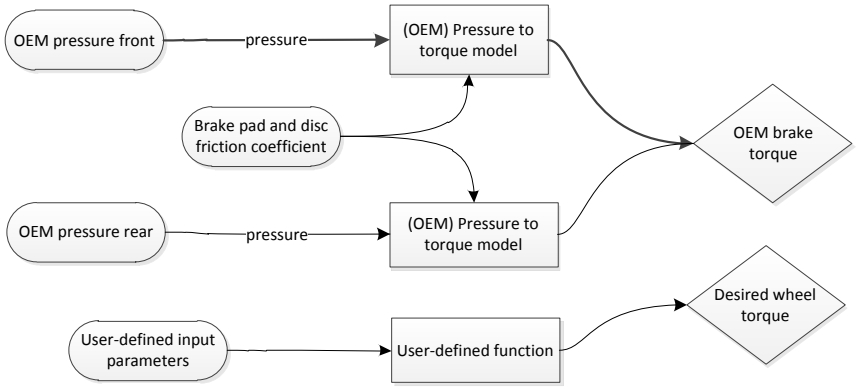

Figure 25. OEM brake torque function in brake demand module

4.5 Motor controller

There are two main objectives of the motor controller model. It needs to saturate the desired torque so that the motor does not exceed its limitations as well as the batteries'. To do this, the model needs to take into account motor and battery behavior. The model outputs two values: the torque at the motor and torque at the wheel. The torque at the wheel will be used for the EHB unit to emulate the torque. The torque at the motor will be sent to the motor model to calculate voltage and current draw. The motor controller's secondary job is to report back the amount of field weakening and the speed of the motor to the motor model.

The breakdown of the motor controller layout is shown in Figure 26. There are 13 inputs, 4 outputs, and 3 modules within the motor controller. The three modules are Inertia model of the drivetrain, Torque saturation model, and Max torque.

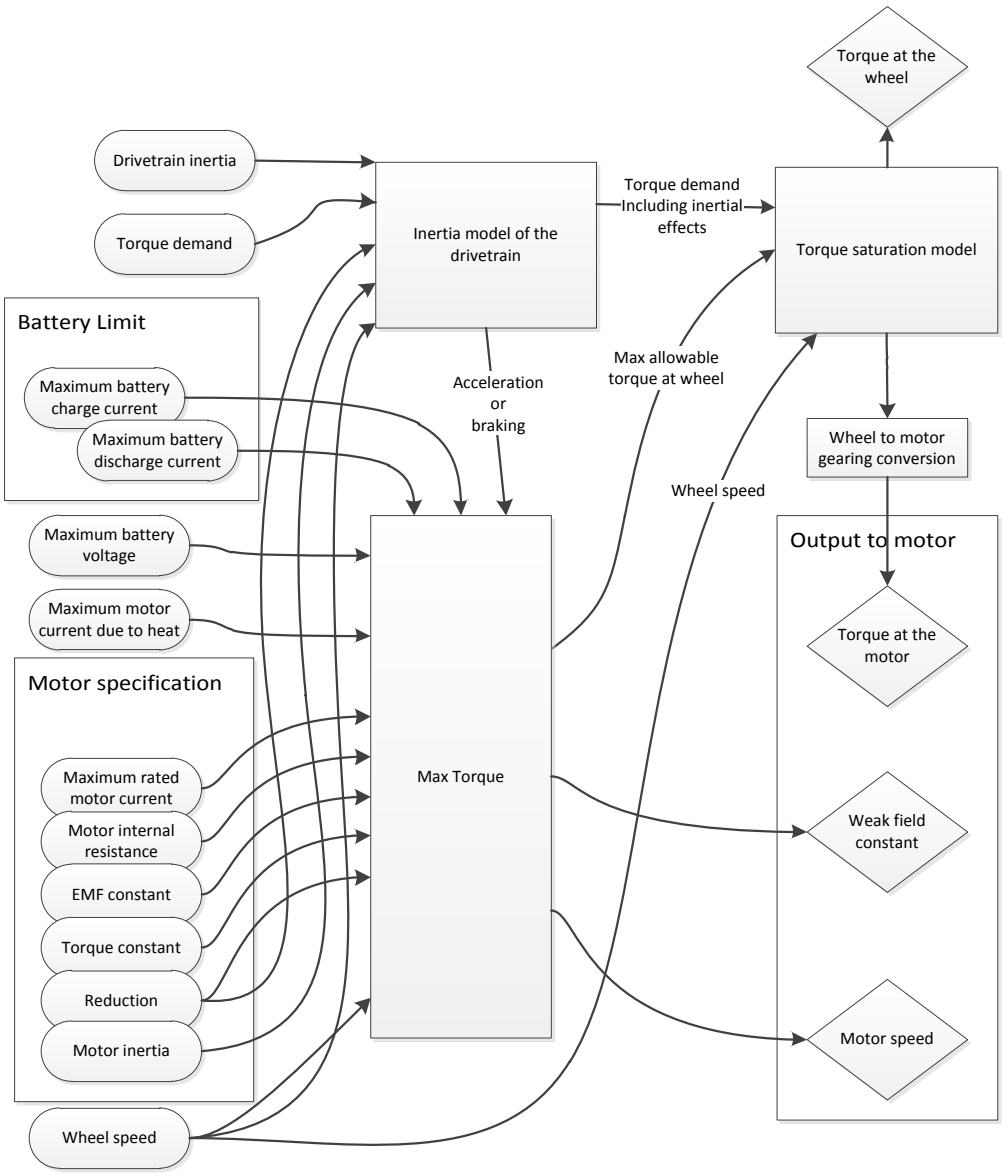

Figure 26. Functionality of motor controller

The inertia model of the drivetrain calculates the total inertia of the entire drivetrain, which includes the inertia of the motor, the wheel, and all the components that connect the two together. The output is the total torque demand which is the inertial torque plus the desired torque.

The desired torque is then inputted to the torque saturation model. The saturation model checks the desired torque to see if it is above the maximum allowable torque at the wheel, which is calculated by the Max torque model.

The Max torque model does all the motor physics calculation. It calculates the maximum torque that the motor can supply at the wheel without exceeding the limits dictated by the battery and motor. It also calculates the amount of field weakening, if any, and the motor speed. A more detailed figure of the motor model is shown below.

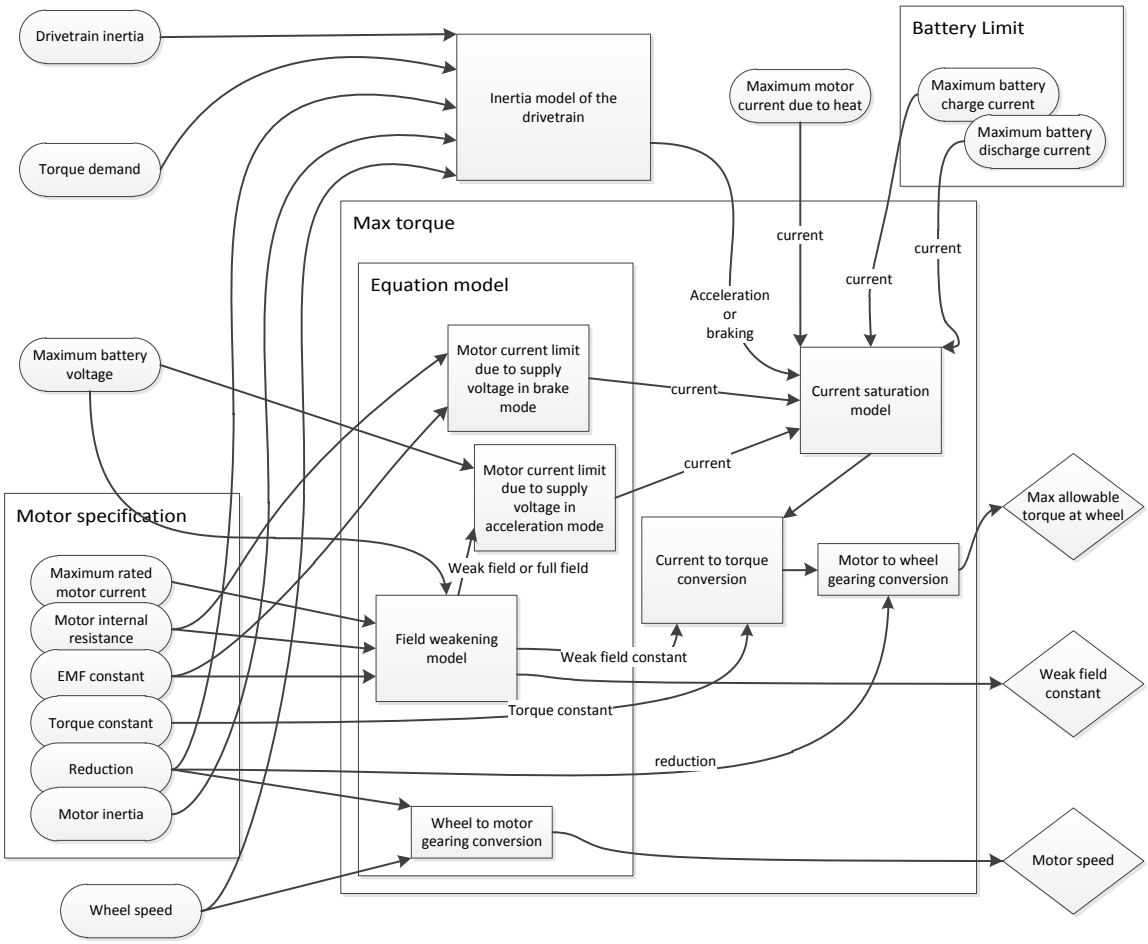

Figure 27. Motor behavior model

In this more detailed view, the Max torque model can be seen as a collection of the equation model, the current saturation model, and the current to torque conversion model. In the equation model, the motor current limit due to supply voltage in brake and acceleration mode is calculated using Equation 3.10. The motor current limit due to supply voltage in brake mode is also calculated using the same equation with V = 0. This is because a negative voltage will produce brake torque while expending energy instead of regenerating it. The field weakening model calculates how much the flux density should be decreased, if need be. It outputs a weak field constant which is defined by the equation below, where E_{peak} is the highest amount of induced EMF possible. This can be calculated using Equation 3.10 at the point boundary between full field and weak field at maximum supply voltage.

$$k_f = \frac{E_{peak}}{k_e \omega}$$

The weak field constant, k_f, can then be used elsewhere to derive the torque/current relationship in the weak field region of the operating regions of the electric motor. All the current limits are then inputted into the current saturation model to output the lowest current limit, which would account for the rest of the current limits. Current to torque conversion is done using Equation 3.13.

4.6 Electric motor

The electric motor model calculates the maximum allowable motor current due to heat as well as the voltage and current it is drawing from the supply. The motor specification, which is entered into this model, is sent to the motor controller block.

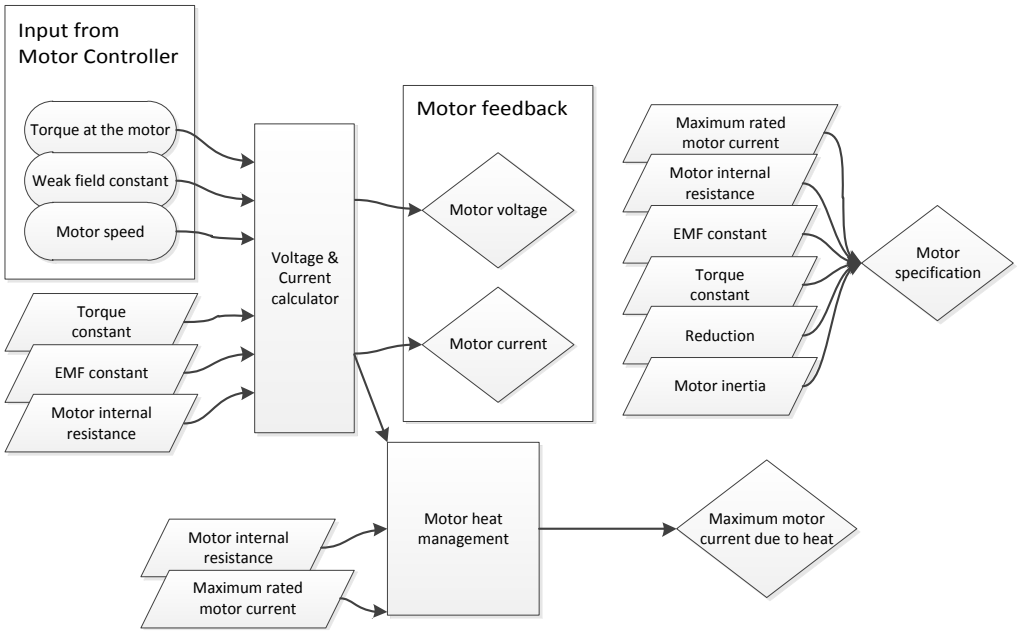

Figure 28. Functional diagram of the electric motor model

4.6.1 Voltage and current calculator

The current is calculated with field weakening taken into account. If the motor is running at full field, then current is calculated according to Equation 3.13. If the motor is running at weak field, then the current is calculated using Equation 4.1 below, where k_f is the weak field constant, I_m is the motor current, T_m is the motor torque, and k_t is the torque constant.

$$I_m = \frac{T_m}{k_f * k_t} \qquad \text{Equation 4.1}$$

The e.m.f. can be calculated using Equation 3.14, and the voltage can be found using the equivalent circuit, Equation 3.15.

4.6.2 Motor heat management

The total amount of heat in the windings is equal to the amount of power absorbed by the resistance of the windings. Below is the equation and the function diagram of the heat management model.

$$\dot{Q} = IV = I^2R$$ Equation 4.1

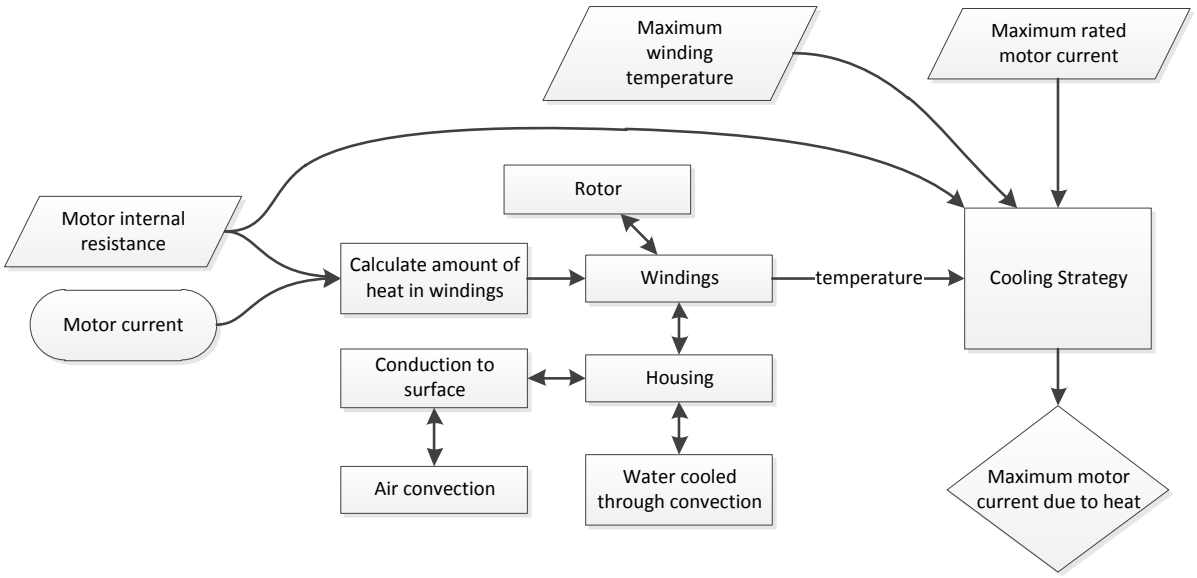

Figure 29. Motor heat management functional diagram

This heat is generated in the windings, spread to the rotor and housing while the housing is being water cooled. The housing also conducts the heat to its outer surface for convection to further cool it. A temperature sensor is attached to the windings in the model, and if the temperature exceeds a predefined maximum temperature, then the cooling strategy model will output a lower maximum allowable current that is fed back to the motor controller.

4.6.3 Power electronics

The power electronics are simply modeled as an efficiency value. It adds up all the power used by the electric motors, and divides that by a pre-defined efficiency. This number is then divided over the battery voltage to obtain the current draw on the battery.

4.7 Battery

Figure 30 shows the overall layout of the battery model.

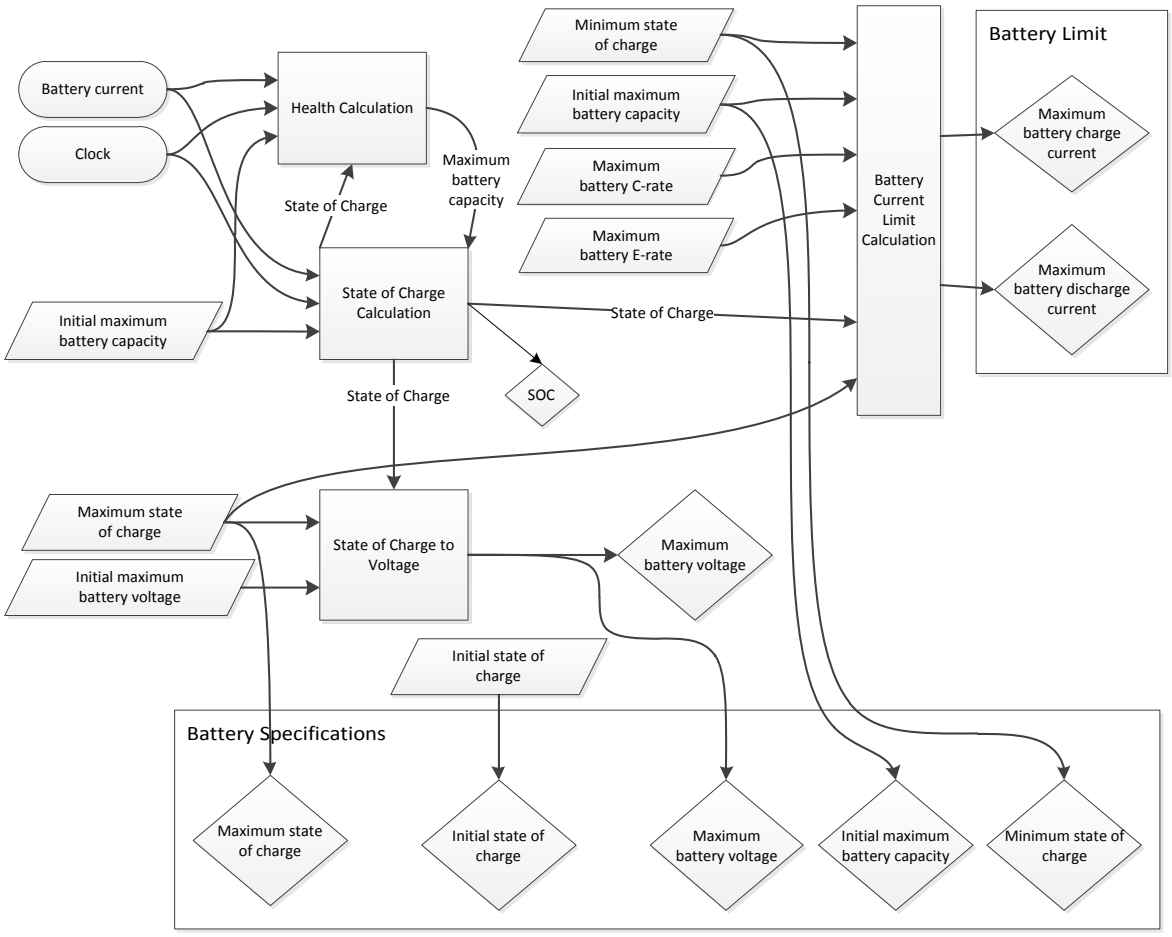

Figure 30. Battery functional diagram

The battery model takes into account all the characteristics of a battery from Chapter 3.4. The battery limit is fed back into the motor controller model, and the battery specification goes to the economy model. The state of charge is not fed back to any other model, but for the user of the software to view and reflect on. Maximum battery voltage is fed back to the motor controller and the power electronics.

The graphs for capacity vs. cycles and the voltage vs. state of charge were scaled from values of a typical Lithium-ion battery (IBT Power Ltd.).

4.8 Drivetrain layouts

Various electric drivetrain layouts can be implemented in the model and 4 were created – front wheel drive with one motor, front wheel drive with two motors, rear wheel drive with one motor, and rear wheel drive with two motors. In addition, an inertia parameter is available for every motor the drivetrain has.

If the simulation is used with the 'Vehicle Simulation' block (Chapter 6.1), then an estimated inertia value should be used. It should include the entire drivetrain from the wheel to the connection to the motor but not the motor inertia. If the program is being

used in the test vehicle, then no inertia should be used since the propulsion torque is calculated from the measured engine torque, which includes the extra torque required to overcome the inertia.

Four drivetrain models were developed. They are front wheel drive with one electric motor, front wheel drive with two electric motors, rear wheel drive with one electric motor, and rear wheel drive with two electric motors. Figures 31 to 34 depict the different drivetrain models.

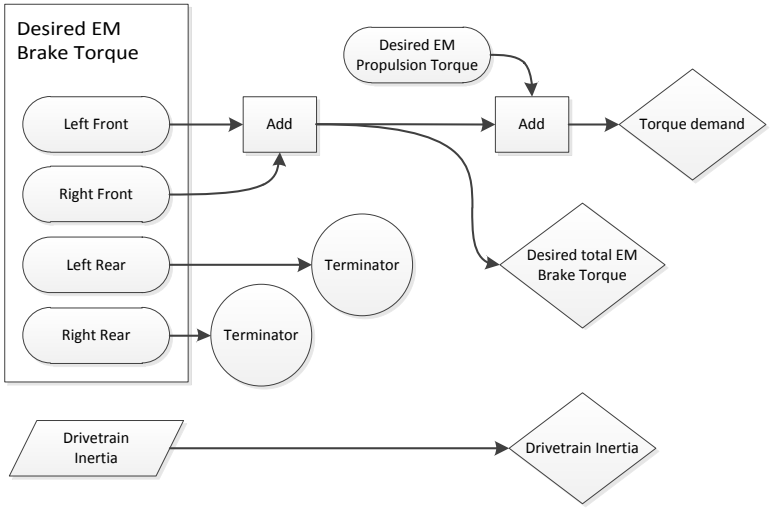

Figure 31. Front wheel drive, single electric motor

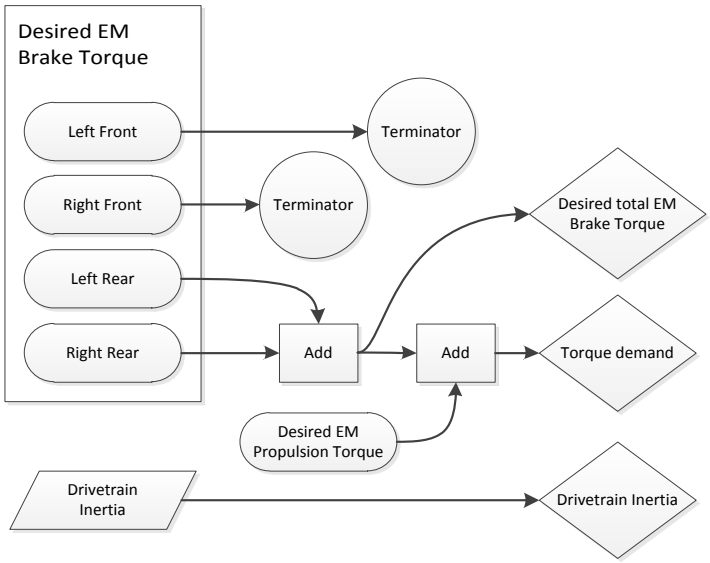

Figure 32. Rear wheel drive, single electric motor

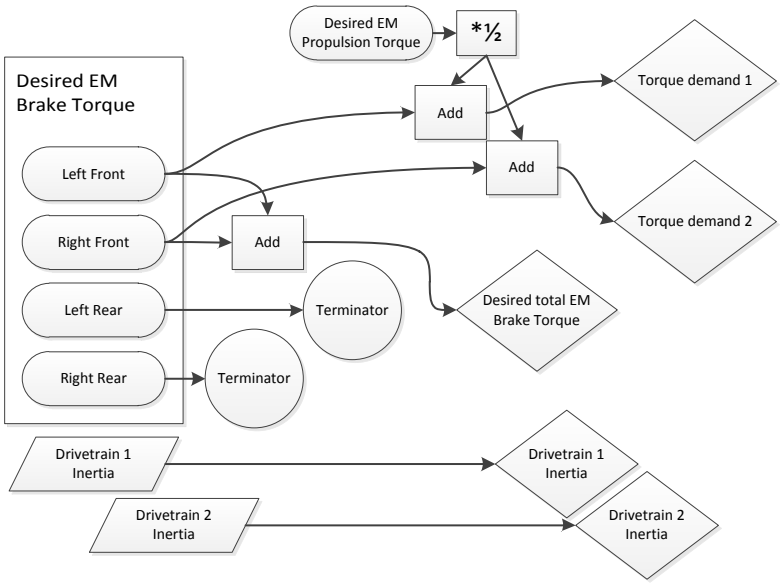

Figure 33. Front wheel drive, two electric motors

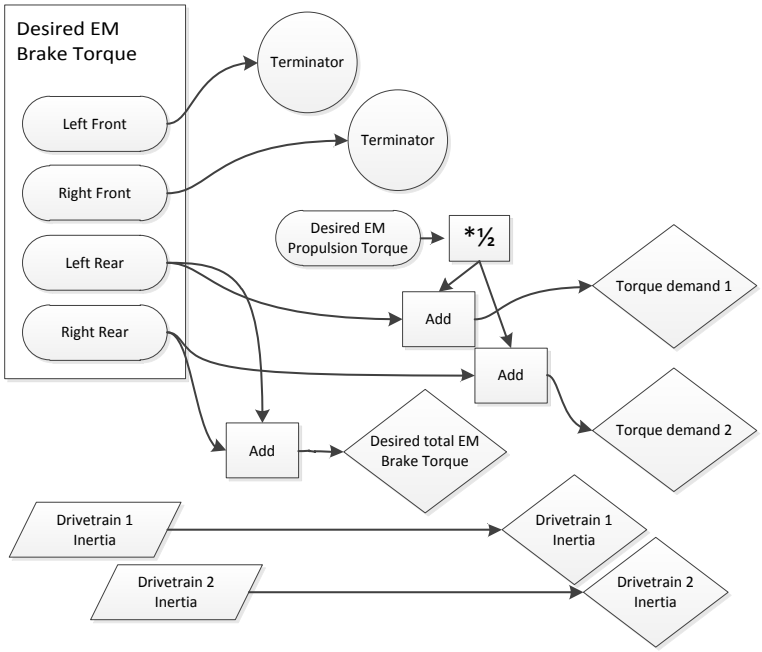

Figure 34. Rear wheel drive, two electric motors

For all driveline cases, the outputs include the torque demand of each electric motor. These torque demands are the sum of the brake and propulsion torque, in case of the driver pushing the brake and the accelerator pedals simultaneously, and are fed into the motor controller module. The desired total EM brake torque output is used when using the vehicle simulation module during software debugging. More on this in Chapter 6.1.

4.8.1 Saturation layouts

Since the modeled electric drivetrain operates in both propulsion and regen mode, the requested wheel torque might be positive (propulsion torque). Since the EHB system naturally can't provide propulsion torque, the torque request from the motor controller module is saturated so that only brake torque passes through. In short, it prepares the torque values to be calculated into pressure at each wheel. It is drivetrain specific so various saturation blocks are created for various drivetrain layouts.

4.9 Vehicle propulsion torque

A propulsion torque must be calculated in order to discharge the emulated battery. To do this, Equation 4.3 was used where T_w is the wheel torque, T_e is the engine torque, ω_e is the engine speed, and ω_w is the wheel speed.

$$T_w = T_e * \frac{\omega_e}{\omega_w} \qquad \text{Equation 4.3}$$

The input is the torque demand for the engine, which is received from the engine management system. The motor model has a gear ratio parameter which is relative to the wheel speed, not the engine speed. Therefore, the variable of interest is wheel torque instead of engine torque. By taking the ratio between the wheel speed and the engine speed, the wheel propulsion torque is calculated. However, the equation does not take into account the inertial loss of the drivetrain. Therefore, the actual torque at the wheels is most likely a bit lower than the calculated one during transient conditions.

The total desired propulsion torque is then used to calculate the electric motor powered portion of that total torque through the use of a hybridization model. A more advanced hybridization model can be implemented as long as it keeps the same input and output of this simple model.

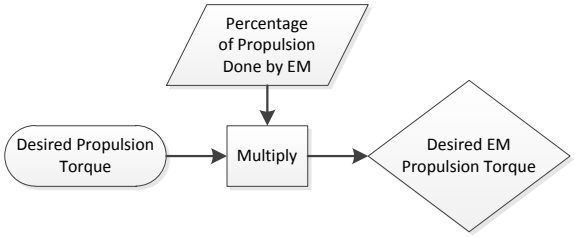

Figure 35. Hybridization model

4.10 Economy

The economy model is used to evaluate the potential gains for regen braking. In the case of a hybrid, the range and consumption being evaluated is of the electric drive system, not the combustion engine.

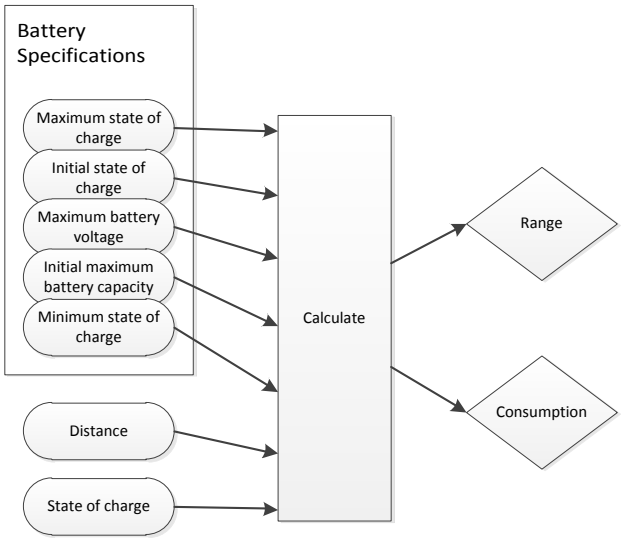

Figure 36. Economy model functional diagram

The 'Calculate' block predicts the vehicle's range and calculates the average energy consumption using the following formulae where R is range, C is consumption, d is distance, SOC is state of charge, SOC_i is initial state of charge, SOC_{max} is the maximum state of charge, SOC_{min} is the minimum state of charge, $V_{b,max}$ is the maximum battery voltage, and $Q_{b,max,i}$ is the initial maximum battery capacity.

$$R = \frac{d}{SOC_i - SOC} * (SOC_{max} - SOC_{min})$$

$$C = \frac{SOC_i - SOC}{100000 * d} * (V_{b,max} * Q_{b,max,i})$$

5 Hardware Layout of the Test Vehicle

In this chapter, the hardware side of the test vehicle is introduced. To start with, the base vehicle is depicted along with an overview of the modifications done and parts added. Next, a safety analysis of the system is done. The EHB system is then described further. The steering knuckle modifications and brake calipers specifications are next dealt with. Lastly, the electric system is presented, including signals, sensors and driver interface.

5.1 Overview

The base for the test vehicle is a 2008 SAAB 9-3. The car is equipped with a V6 Turbo engine and a manual gearbox. The specifications were chosen to be similar to that of the current test vehicle at Chalmers, which will undergo the same modifications as the SAAB car. By having the same equipment, the results gathered by the two cars can be compared.

An overview of the modifications made is shown in Figure 37.

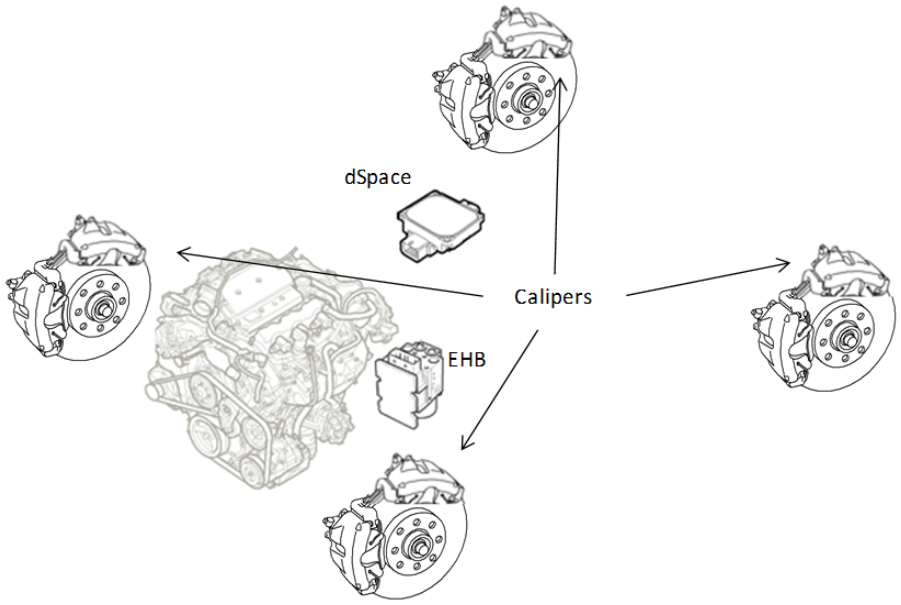

Figure 37. Overview of test vehicle modifications

An extra brake caliper is added to each corner of the car. All four steering knuckles are modified to house the new calipers while retaining the standard calipers. The brake modifications are described in detail in Section 5.4.

An EHB system is mounted in the engine compartment, in the space allocated for the battery. The battery itself is moved to the trunk. The main parts of the system are the EHB unit, the brake fluid reservoir and the wiring. The EHB system is described further in Section 5.3. Brake tubing and lines are fitted, connecting the EHB unit to the calipers.

A dSpace MicroAutoBox II control board is mounted in the cabin. It communicates with the EHB unit, the in-car CAN bus and some additional sensors. The additional sensors include a brake pedal travel potentiometer and two brake pressure sensors mounted on the standard brake system. Realized EHB pressures are received from the EHB unit. The software for the dSpace is downloaded from a laptop computer, which

has a special computer table set up at the front passenger seat. Complementing the computer controls is a box with physical switches, which activates/deactivates the EHB system and provides configurable hardware functionality. The dSpace computer, signal gathering and driver interface are all discussed in Section 5.5.

5.2 System safety analysis

In this section, an analysis of the system functions is done to ensure that the final vehicle is safe to use on both the test track and public roads.

5.2.1 Safety requirements

The test vehicle will primarily be used on dedicated test tracks. An important consideration is that it should still be capable of driving to and from the tracks on public roads. This desire results in two major requirements on the test vehicle:

- The original friction brake system should be retained, completely and without modifications.
- The EHB system can be totally electronically disengaged.

If fulfilled, these two requirements should enable the test vehicle to function exactly as a standard vehicle when going on public roads.

While the safety in the transportation mode is reliant on keeping the standard vehicle functions intact, the safety level during operating mode also depends on the predictability of the added functions. Arguably, the precision of the functions is a safety-related aspect. If the brake output differs in size, time response or any other respect from the requested output, unwanted situations may occur. Having the system properly calibrated is therefore not only of interest for precision in data sampling, but also for the safety of the user. The calibration methods used for the test vehicle are presented in chapter 0.

In a production car, safety-critical signals are made redundant, with observers controlling the function. Due to the software type and the fact that the program is to be modified by the end user, proper signal security is difficult to implement. For the test vehicle software, the error handling is limited to making sure that the output torque values are within the operation range of the EHB, and that they are saturated if not.

A user guide is put together to inform the end user of precautions to take when using the car. The aim is to provide a short, clear and informative paper with procedures for both putting together new software models and executing them in the test vehicle.
The guide can be found in the vehicle.

5.2.2 Hazard analysis

Errors in a safety-critical system might lead to a hazard or, in worst case, a mishap. The brake system implemented in the test vehicle is a safety-critical system. Consequently, a systematic approach should be used to maintain the safety integrity of the system. The engineering branch concerning risk management is called system safety engineering. System safety should not be confused with reliability. The

intention of system safety is not necessarily to minimize the number of breakdowns, but rather to ensure that the effects of the breakdowns do not lead to hazards.

A part of system safety engineering is to identify, evaluate and control potential hazards of the system, called hazard analysis. This approach was deemed to be suitable to analyze the system safety of the test vehicle. It provides useful insights in the system as a whole whilst being more manageable than the large effort of a complete Failure Mode and Effects Analysis (FMEA) or a fault tree analysis. The hazard analysis is consistent with the ISO 26262 "Road Vehicles – Functional Standard".

The hazard analysis was carried out in a number of steps. First, a block diagram of the system and its boundaries was drawn. By understanding all involved parts and functions, any unintended effects can be determined. The unintended effects were compiled in a sheet, listing the parts/functions and the effect at different function states; total loss, incorrect activation (more/less than expected or in the wrong direction), unintended activation, or locked activation. Each effect was linked to one or several hazards from a predefined list of vehicle hazards. Each hazard is in turn associated with a risk. The risk scale is called ASIL and the value is determined from the severity, likelihood and controllability of the hazard.

Two important conclusions were drawn from the analysis:

- For functions that may lead to a complete or partial loss of brake torque, falling back to the standard brake system is sufficient to avoid hazards.
- The emergency switch needs to be able to disengage all functions that may introduce unwanted brake torque and vehicle lateral motion, if no suitable redundancy can be accomplished. Shutting down the EHB power is sufficient to cover potential hazards.

Hence, the result of the hazard analysis is consistent with the requirements previously put up in Section 5.2.1, as long as the emergency switch is able to completely disengage the EHB system.

5.3 EHB system

The EHB system used is a Mercedes-Benz Sensotronic Brake Control (SBC) unit. It was introduced in the 2003 SL-class (R230). Other models to use the SBC system is the 2003-2005 E-class, CL, CLS, SLR and the Maybach. It was dropped in the high-volume E-class due to reliability problems. The problems were related to the pump motor being worn out on cars with high mileage or high frequency of brake operation. The reliability issue is of long-term use nature and deemed not a problem for the test vehicle.

5.3.1 Technical overview

One main feature of the selected system is the ability to adjust both front to rear and side to side brake distribution. Effectively, this gives possibility to control each brake caliper individually. Another feature is the precision and accuracy of the system. In the vehicles using SBC, a so called soft-stop function is implemented. As the driver brakes and the car approaches standstill, the brake pressure is gradually decreased to

give a smooth coming to a stop. The actual performance of the EHB as implemented in the test vehicle is further analyzed in Section 6.4.

The original SBC system consists of three main components: Brake Operating Unit (BOU), wheel speed sensors and Traction System Hydraulic unit. Traction System Hydraulic unit is the part previously called the EHB unit. Figure 38 gives an overview.

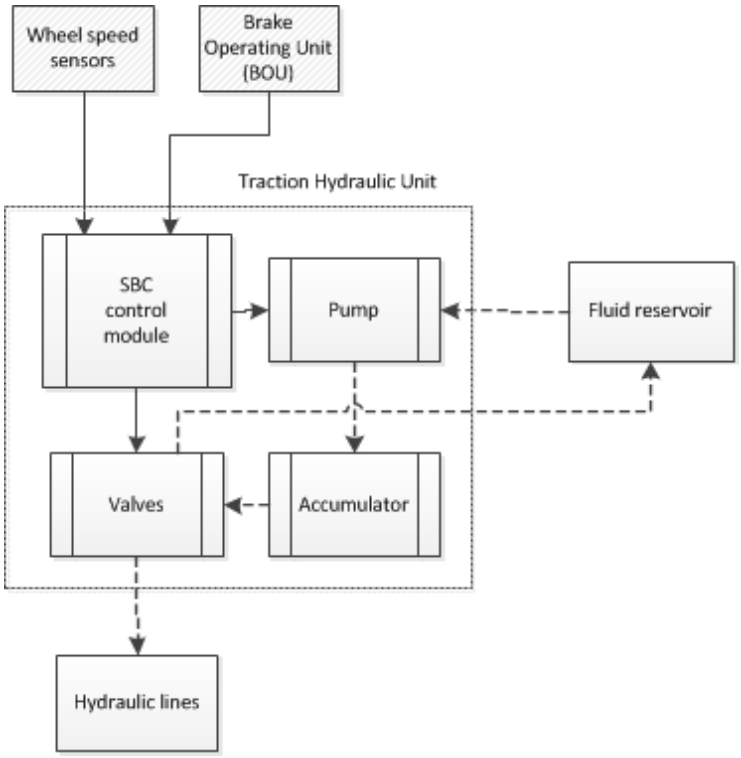

Figure 38. Overview of EHB Traction System Hydraulic unit

In the Mercedes, the BOU is the device measuring the brake demand of the driver. Even though this unit is not used in the test vehicle, the BOU pedal sensor remains connected to the wiring harness to avoid diagnostic errors. The BOU usually houses the brake fluid reservoir. Since it is not used in the test car, the reservoir is directly connected to the EHB unit fluid supply and return ports.

The wheel speed sensors are also unused but connected to the harness to avoid diagnostic errors. They are packaged in one side of the engine bay, on top of the front left fender.

The Traction System Hydraulic unit consists of a control module, electronic valves, a high pressure charge pump and a pressure accumulator. The pressure accumulator is dimensioned to maintain an operating pressure of 160 bar. The complete unit is packaged where the SAAB battery originally sits. It is not mounted in rubber bushings and makes a loud but harmless noise when pumping fluid.

In the original car, there's a private Controller-Area Network (CAN) bus between the SBC control module and the Electronic Stability Program (ESP) control module. ABS, ESP and Brake Assist (BAS) requests are sent over this bus. The SBC unit monitors the brake request from the BOU and sends it to the ESP module. The ESP module calculates appropriate pressures, which are sent to the SBC. The pressure values are set and actual values signaled back to the ESP unit.

In the test vehicle, the private CAN bus is taken over and used both to request brake pressure and to gather information from the system. TNO, a Dutch technical research institute, provided the software to achieve this. The availability of the TNO-software was, together with the technical properties of the EHB system, the major reasons for choosing the Mercedes SBC system for the test vehicle.

5.3.2 Hydraulic layout

The hydraulic layout of the original SBC system is displayed in Figure 39.

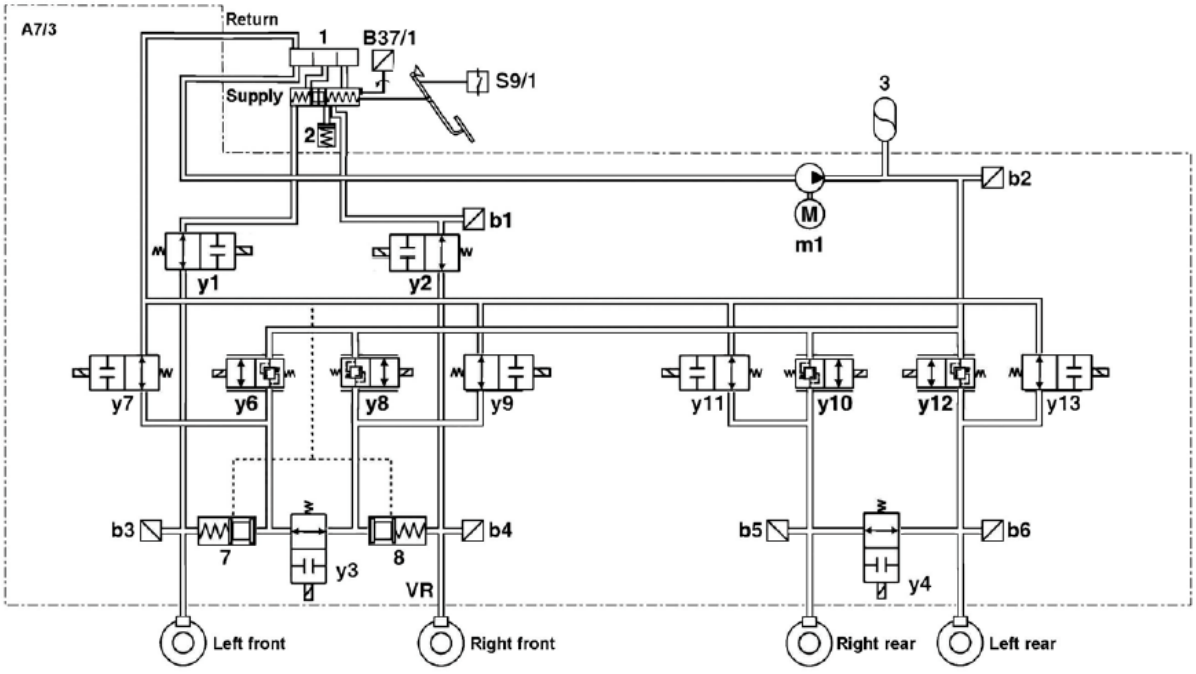

Figure 39. Hydraulic architecture of original SBC system

The SBC system consists of two hydraulic circuits; a main circuit and a backup circuit. The backup circuit is engaged when errors occur or when the system is switched off. Since the BOU is not connected, the supply line from the brake fluid reservoir is split to feed brake fluid to the backup circuit. Components m1 and m3 is the pump and pressure reservoir respectively. Components b1 to b6 are pressure sensors. Component b2 monitors reservoir pressure and turns pump on/off to maintain working pressure in the main circuit. Aside from measuring the brake pressure for each corner, the brake pressure of the backup circuit is measured. Components y1 to 13 are control and balance valves. These are electronically controlled by the SBC control module. There are three distinctive modes of operation; Pressure apply, pressure hold and pressure release. In all cases, the inlet and outlet control valves are energized in conjunction with the high pressure pump to give desired effect. By also utilizing the balance valves, the brake pressures can be individually modulated.

5.3.3 Bleeding the EHB brakes

As usual, bleeding is done by connecting a pressure bleeder to the fluid reservoir and opening the bleeder valves at the calipers. The EHB unit is turned on and off to get air out of both the main and the backup circuit. Needless to say, the EHB unit has to be

operational in order to run the pump and build up pressure in the main circuit. This is comparable to putting pressure on the brake pedal in an ordinary car.

5.4 Steering knuckles & brakes

At each corner of the car, an extra brake caliper is mounted. The main requirement is that they should be able to lock the tires on dry asphalt. Using a simple Matlab program, the necessary caliper piston area is calculated from the EHB operating pressure, the car weight, disc size and estimated pad friction coefficient. The results suggest that a two-piston caliper should have a piston diameter of around 40/25 mm front/rear. While a bigger piston size gives more safety margins and less stress on associated components, it will also give worse caliper response. Since the objective of the extra calipers on the test vehicle is to emulate the quick response of electric motors, as small calipers as possible are recommended.

For caliper selection, not only should they have the correct piston diameter, but it is also necessary to consider how to package them inside the wheels. The standard steering knuckle assemblies are not designed to house dual calipers. Also, the extra calipers should fit over the standard discs. Considering both the packaging and the manufacturing, a radial mounted caliper is chosen. For the front, AP Racing CP5317 calipers are used. For the rear, AP Racing CP5316 calipers are used. They are virtually the same caliper but with piston diameters of 41,28 mm and 38,10 mm respectively.

Two different solutions are chosen for the front and rear caliper mountings. At the front, a flat face is milled on the knuckle, onto which mounting brackets are bolted. At the rear, a mounting plate is bolted onto the knuckle between knuckle and the wheel hub/disc. Some material is taken off the knuckle. Figure 40 (left and right) show the modifications made; the caliper mounting bolts giving an indication were the extra calipers are situated.

Figure 40. (left) Front caliper mounting, (right) Rear caliper mounting

The chosen calipers support brake pads from numerous different manufacturers. A number of brake characteristics are associated with the pad material; noise, disc wear and brake power, to name a few. One important consideration is to have a pad that keeps the friction as constant as possible across the intended span of operating temperatures and pressures. The chosen pads are retailed as APF405, but are manufactured by Federal-Mogul. Part name is FER3432F. The pads are the same for the front and the rear. Data for the pads was given by the manufacturer. The specific heat and thermal conductivity is shown in Figure 41.

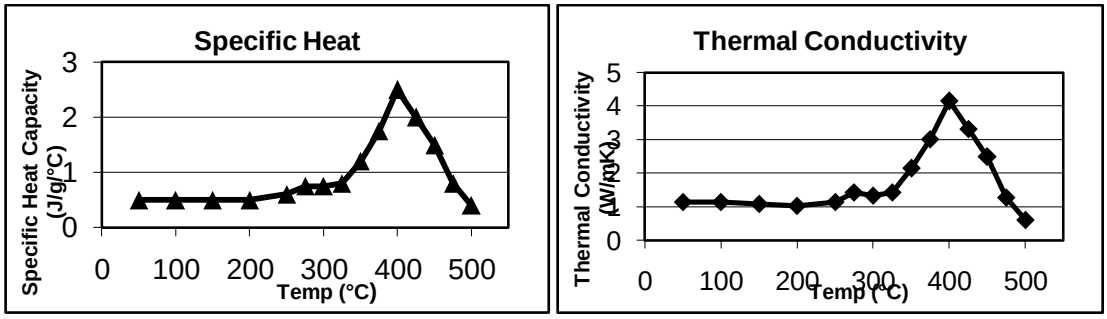

Figure 41. Specific heat (left) and thermal conductivity (right) of the AP Racing brake pads

The brake pad material has a specific heat which varies depending on its temperature. Figure 41 (left) shows that as the temperature rises to 400℃, it takes more heat to raise the temperature of the brake pads. For temperatures higher than 400℃, the specific heat decreases to previous levels. Figure 41 (right) shows a similar relationship for the thermal conductivity.

An indicative curve for the friction coefficient vs. temperature behavior was also supplied. However, for better accuracy and to take into account installation and bedding-in factors, the pad/disc friction variation over temperature and pressure is calibrated in the final vehicle, Section 6.3.1.

Of interest is also the specification of the standard brake system pads. The part names are T4139/T4140(4GD) for the front/rear pads respectively. Similar data to that of the EHB pads was obtained from the manufacturer TMD Friction. As with the EHB pads, the standard pad/disc friction is also analyzed during testing.

5.5 Signals and sensors

5.5.1 Electric system overview

The core of the electric system is the dSpace box. It is packaged in the front passenger foot well, covered by a metal plate. This computer executes the user programs and communicates with the EHB and the available sensors and signals. The model used is a MicroAutoBox II, version 1401/1505/1507. It has four CAN interfaces, two of which are connected to the EHB unit and the vehicle bus respectively. The use case analysis shows that extra electronic units may be connected, which could be done in any of the two remaining CAN interfaces. Additionally, the box has 16 analog inputs, which is more than sufficient for the initially utilized sensors and triggers. On the software side, the dSpace is provided with Real Time Interface (RTI), RTI CAN blockset, Power PC Compiler and ControlDesk. These programs enable the user to build and execute Matlab/Simulink programs in real-time on the dSpace platform. Figure 42 gives an overview of the electric setup.

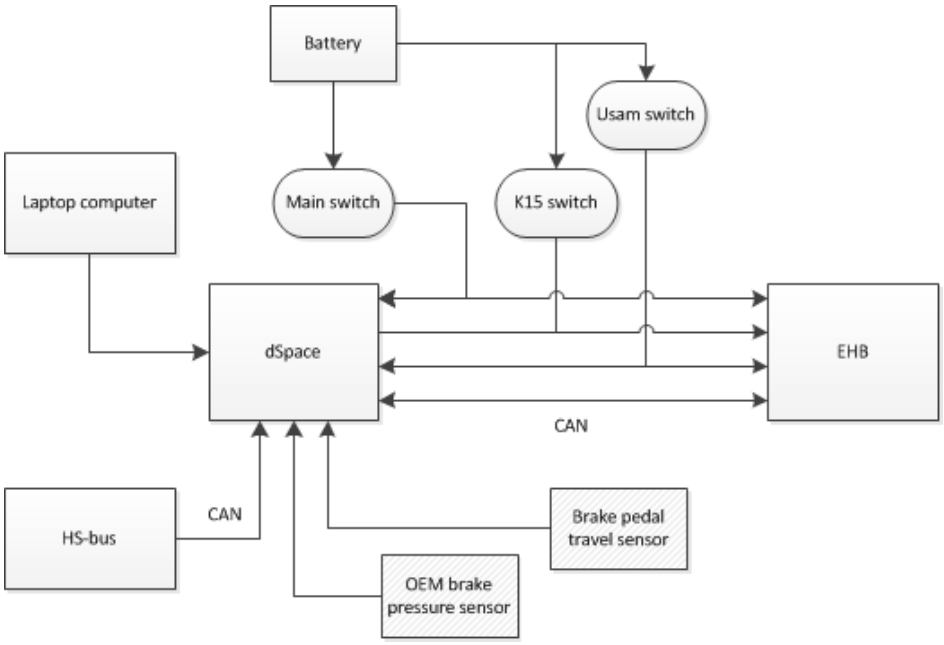

Figure 42. Electric architecture of EHB and control system

The dSpace sends requested brake pressure for each wheel in bar, and receives achieved pressure values along with status signals. Both units are connected to the battery power supply, the connection being controlled by an emergency switch. Additionally, the test vehicle must have ignition on for dSpace to power up. Communication with the laptop computer is done via an Ethernet cable.

The dSpace and the EHB unit are supplied with two simulated vehicle signals present in the original Mercedes integration environment; the Usam signal and the K15 signal. The Usam signal is the wake up signal for the EHB, in the original vehicle triggered for instance by a door being opened. When this signal is supplied in the test vehicle, the EHB will operate autonomously, i.e. it will react to the BOU travel sensor but not to requests sent by the dSpace. The K15 signal indicates the ignition position in the original vehicle. When this and the Usam signals are both triggered in the test vehicle, the EHB will respond to request sent by the dSpace. The activation signals are presented to the dSpace box as well, to activate the software program at the same time as the EHB.

5.5.2 Driver interface

The driver interface is shown in Figure 43.

Figure 43. Test vehicle control panel

Controlling the Usam and K15 signals are switches (2) and (3) on the panel. Keeping their function in mind, these are the on/off switches for the EHB. Also present is an on/off switch for the dSpace (1), the emergency switch (top end) and four linear, non-stepped potentiometers (5-8). The software function of these can be defined by the user. Also present on the panel is a stepped switch (4), a trigger switch (bottom end) and an input port for an external switch (bottom end). However, these are at the time of writing not yet connected. All in all, for a computer program to create brake torque, intentionally or unintentionally, all of the following statements need to be true:

- Emergency switch off
- dSpace, K15, Usam switches on
- Ignition on
- Laptop connected and set up correctly
- Software executed

If any statement is untrue, no brake torque will be provided.

5.5.3 Gathered vehicle parameters

The use case analysis pointed out certain vehicle parameters to be gathered. The majority of these are already present in the standard car. Signals sourced by the different electronic units in the vehicle are shared on a common communication bus, the High-Speed bus (HS-bus), using the CAN protocol. The dSpace is connected to the HS-bus through one of its CAN interfaces and can thereby sample all shared information. Parameters that are initially set up to be available for the test user include vehicle speed and acceleration, wheels speeds, engine torque and speed, accelerator and steering wheel position. Needless to say, the list can be expanded to include any available signal with a known CAN identifier. The standard yaw rate sensor is replaced with one from the SAAB 9-3X, which provides longitudinal acceleration as well as lateral acceleration and vehicle yaw rate to the HS-bus.

Some requested parameters are however not available as standard. An analog travel sensor is mounted on the brake pedal. This is a SAAB BASS unit, used in the new generation 9-5. Knowledge of the standard brake system state is also requested. Two pressure Bosch 0265005303 sensors are therefore mounted; one on the front circuit and one on the rear circuit. Both the pedal sensor and the pressure sensors are connected to the analog interface of dSpace.

5.5.4 Connections to test vehicle

A Simulink software was provided by TNO for basic controlling of the EHB. It consists of an S-function which transmits and receives CAN signals to and from the EHB unit. The S-function is depicted by the EHB unit in Figure 44. This allows pressure signals to be sent to the EHB and pressure readings to be received without the knowledge of the EHB's CAN information such as identifiers, starting bit, length, etc. The multiport switch on the bottom left of Figure 44 chooses four different braking programs, which sends various brake pressures signals to the S-function. Therefore, minimal modification to this program is all that is needed to send custom pressures to the EHB.

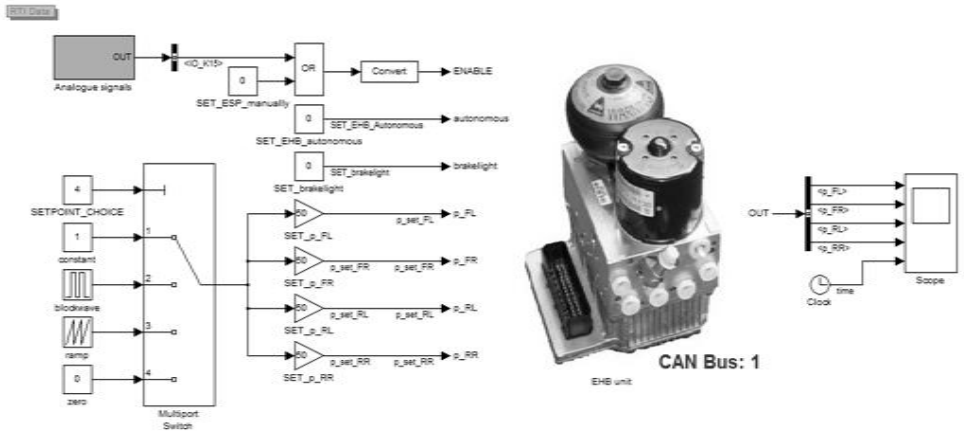

Figure 44. TNO Simulink software that transmits and receives CAN signals to and from the EHB

For the other CAN signals that are to be received from the car, the CAN information is needed to read the encoded CAN messages. For the analog signals, the only information required is the converter and channel number of where the signal is connected to the dSpace computer. Fortunately, for both CAN and analog signals, the dSpace software provides Simulink blocks which allow this information to be entered easily, shown in Figure 45, Figure 46 and Figure 47.

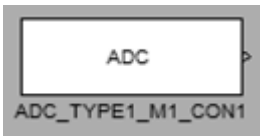

Figure 45. dSpace analog signal block

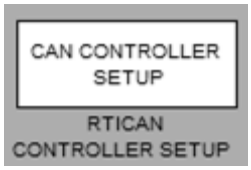

Figure 46. dSpace CAN controller block

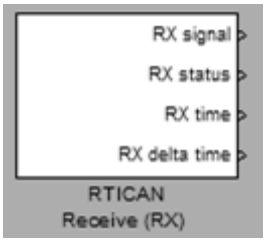

Figure 47. dSpace CAN receive block

For ease of handling all the CAN information, a DBC file was obtained for the Saab 9-3, which was then loaded into the CAN controller block. The CAN receive block can then use the file loaded to load messages from a specified CAN identifier.

6 Calibration and Validation of Test Vehicle

Testing is required both to calibrate software parameters and to ensure adequate function of the final product. Firstly, the method used to debug the software is presented. Secondly, the hardware equipment used during calibration and testing is described. The calibration method for all calibrated function is then described along with associated results. Lastly, the final performance of the test vehicle is presented along with notes from the test session.

6.1 Software debugging

The vehicle simulation model allows testing of the entire software without the need for a car. It makes the early process of evaluating new control ideas easier and faster. It takes a simulated pedal travel and a specified maximum torque to output a desired propulsion torque.

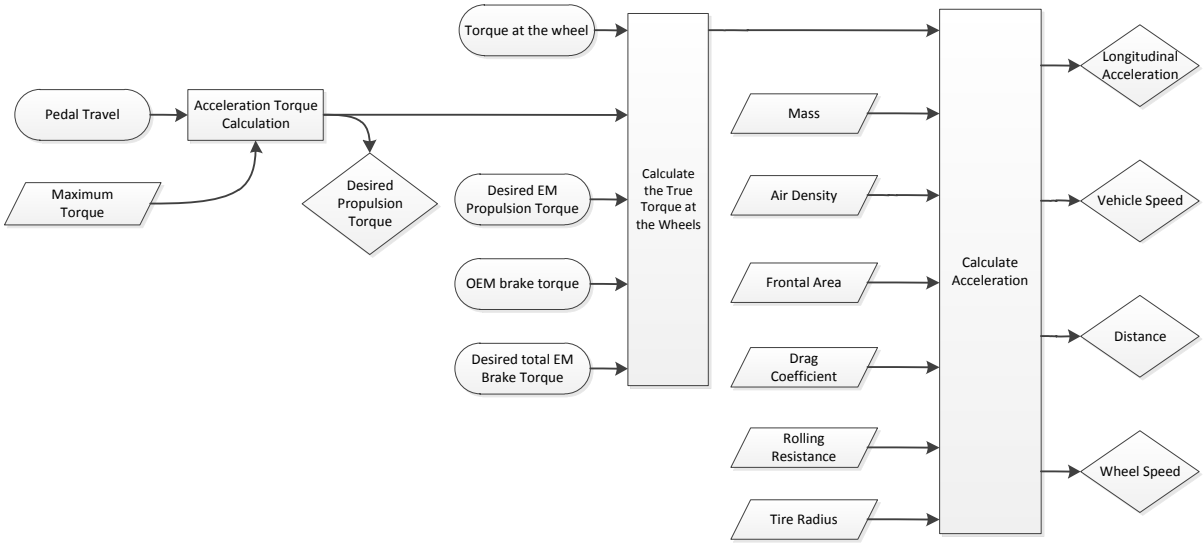

Figure 48. Vehicle simulation model functional diagram

The desired propulsion torque, along with the saturated EM torque at the wheel, the desired EM propulsion torque, the OEM brake torque, and the desired total EM brake torque are used to calculate the real torque at the wheels. The desired torque will always be greater than or equal to the real torque output in magnitude due to the limitations of an electric motor, and there is also torque coming from the OEM brakes and the combustion engine. This forces the calculation of the real torque at the wheels to take many factors into account.

The tire rolling resistance and air resistance will then be subtracted from the real torque calculated. This will lead to the calculation of acceleration, and with integration, linear velocity, wheel speed, and distance.

6.2 Test equipment

Two predominant tools are used for the calibration and validation of the test vehicle. They are described further in the following subsection.

6.2.1 HIL-rig

A hardware-in-the-loop (HIL) rig is used to calibrate software functions. The rig was specified partly with the master thesis in mind. It enables measurements of rotational speed, torque, brake line pressure and disc temperature to be taken. Figure 49 shows the overall layout of the rig.

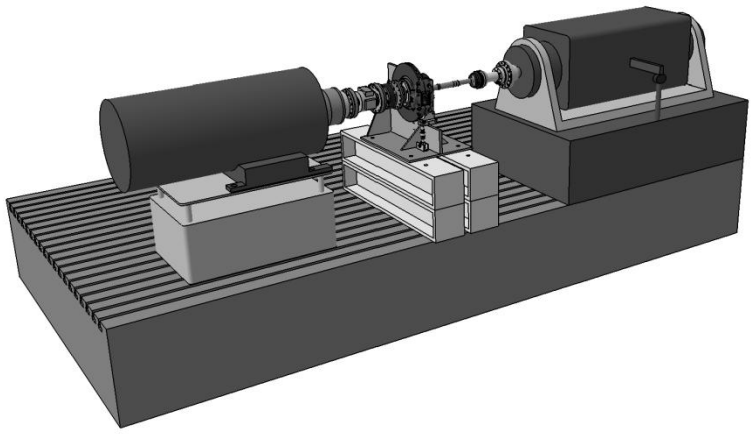

Figure 49. HIL-rig components

The right electric motor simulates the road load, while the left motor simulates electric motor braking. They drive a common axle, at which torque is measured at three places; at the road load motor, at the caliper mount and at the braking motor output shaft. The braking motor was going to be used as a reference braking source for the friction brakes to be compared to. The temperature of the brake disc is taken by a moveable Infrared (IR) sensor. The motor speed is given by the road load motor controller, while the brake line pressure is recorded by a Bosch pressure sensor. The caliper brake pressure is put on manually using a separate brake pedal and master cylinder assembly. The caliper used is the AP CP5217 used at the front of the test car. However, the correct brake pads were not available during the thesis, which narrowed down the work in the HIL-rig to calibration of the disc heat convection.

6.2.2 Torque wheels

Torque wheels enable the torque of the wheels around its axis of rotation to be measured during driving. The torque wheels are used to verify the correctness and performance of the final vehicle installation, calibrate software functions and to gather information on the standard brake system as this is not put in the HIL-rig. During measurement, the standard wheels are replaced by the torque wheels altogether. The model used is Kistler RoaDyn, shown in Figure 50.

Figure 50. The torque wheels used

For the particular case of the test vehicle, new hub adapters were manufactured to fit the given bolt pattern. The registered data is transmitted wirelessly from the torque wheels to a control unit. This imposes a time delay of 244ms, which was taken into account during measurements. The data is transferred to the dSpace computer for logging using an analog cable.

6.2.2.1 Calibration of torque wheels

The torque wheels were supplied with calibration factors. However, a calibration test was carried out to verify these. Firstly, the total weight of the car was measured. The car was then put on a steep hill. The vehicle was aligned using the lateral acceleration value, the car being straight when this turned zero. Figure 51 shows the car on the hill.

Figure 51. Calibration of torque wheels.

Since the two torque wheels were both put on the front axle of the car, the front EHB brakes were applied to hold the car still. Thereby, all longitudinal force was taken by the measured wheels. The longitudinal acceleration was then measured. Multiplying this value with the vehicle mass and the tire radius gave a calculated wheel torque. The calculated values were compared to data gathered from the torque wheels. The results are presented in Table 2.

Table 2. Torque wheel calibration results

Experiment	Long. Acc. (m/s^2)	Calculated torque (Nm)	Measured torque (Nm)
1	1.90	565.8	536.0
2	1.88	559.8	547.0
3	1.95	580.7	561.0

The difference might be due to the weight transfer giving a deflection of the springs, which in turn gives a slight angle between the accelerometer and the road surface. However, the values were close enough to trust the manufacturer-supplied calibration factors.

6.3 Calibrated parameters and method

Calibration method and results are here presented for each calibrated parameter or function. For all in-vehicle tests, the torque wheels are used to measure the brake torque at the wheel. The brake pad and disc temperatures are taken with a handheld thermocouple.

6.3.1 Friction coefficient of EHB brakes

The disc/pad friction coefficient of the EHB system is calibrated in the vehicle. The following driving cycle was used.

Figure 52

Table 3

Location	Description
A	Measure brake pad and disc temperature, accelerate to speed
B	Brake with constant pressure
C	Stop and measure brake disc and pad temperature

Constant brake pressure is applied and the measured torque can be used to calculate the friction coefficient, using Equation 3.1. The average friction coefficient and average temperature during a run was taken. By repeating the test for a span of starting temperatures, a friction vs. disc temperature curve was put together. Figure 53 shows the friction curve for the front EHB brakes.

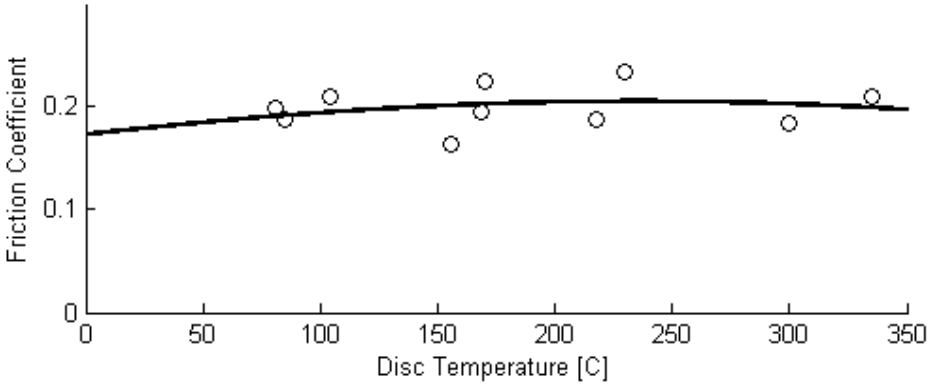

Figure 53. Friction coefficient vs. disc temperature.

As can be seen in Figure 53, a relationship between the friction and the disc temperature exists. To complement this result, the friction coefficient was plotted as a function of pad temperature, Figure 54.

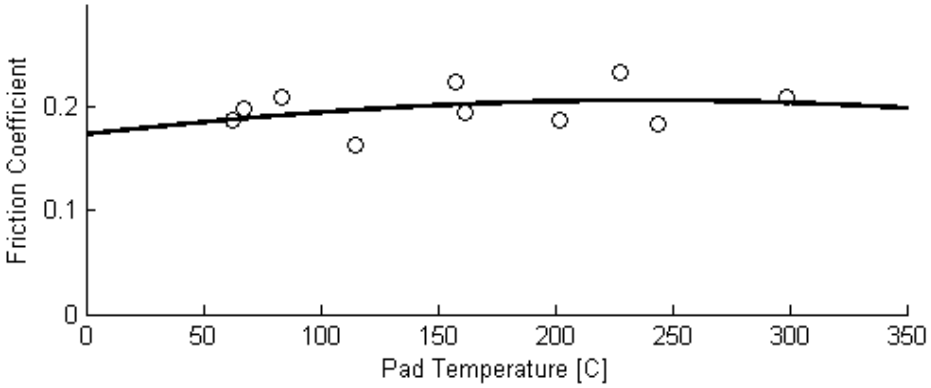

Figure 54. Friction coefficient vs. pad temperature.

In Figure 54, the friction coefficient displays a similar parabolic behavior as shown in Figure 53. It should be noted that the data points represent the average friction and temperature during the braking instance. Figure 55 shows the raw data from the same calibration tests.

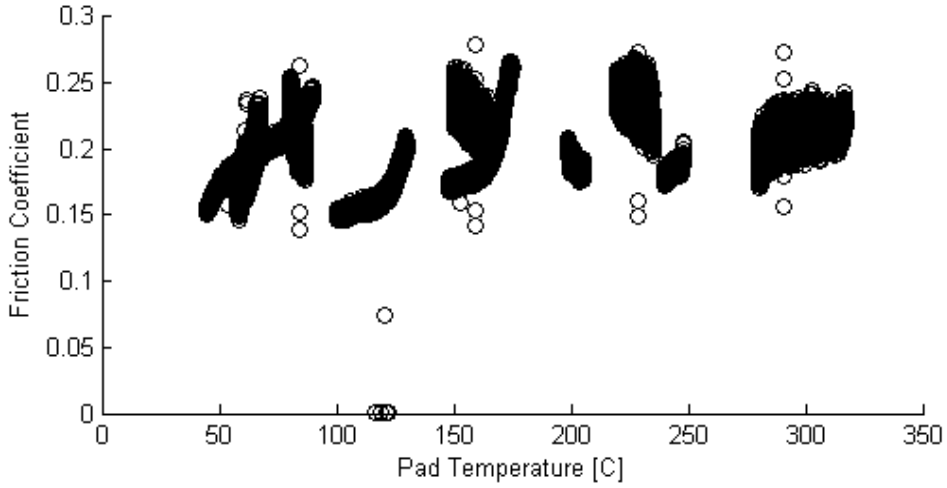

Figure 55. Friction coefficient vs. pad temperature, raw data.

Together with the corresponding data for the disc, it was noted that during the braking phase, the brake pad can be heating up while the brake disc is cooling down, or vice versa. However, since the average is used for creating the friction vs. temperature curves, no difference is seen between the pad and disc graphs.

Noteworthy is that the EHB friction coefficient is around 0.1 lower than specified by the manufacturer. Noticing this, the bedding-in procedure of the EHB brakes was redone. However, this didn't give any change in friction level. Still, the braking power of the EHB system it is enough to lock the wheels on dry tarmac.

The driving cycle was repeated for different brake pressures to analyze the influence of pressure on the friction coefficient. No correlation was found and the brake pads are therefore said to be dependent on the temperature only.

No tests on the rear EHB brakes were conducted, due to problems arising with the torque wheel adapters. Since the brake pads are the same for the front and rear for the EHB system, similar thermodynamic properties can be expected for the rear EHB pads as for the front.

6.3.2 Friction coefficient of OEM brakes

To analyze the friction coefficient of the standard brake system, the same procedure and driving cycle was used as for the EHB calibration, described in Section 6.3.1. Figure 56 shows the friction curve as a function of the disc temperature for the front OEM brakes.

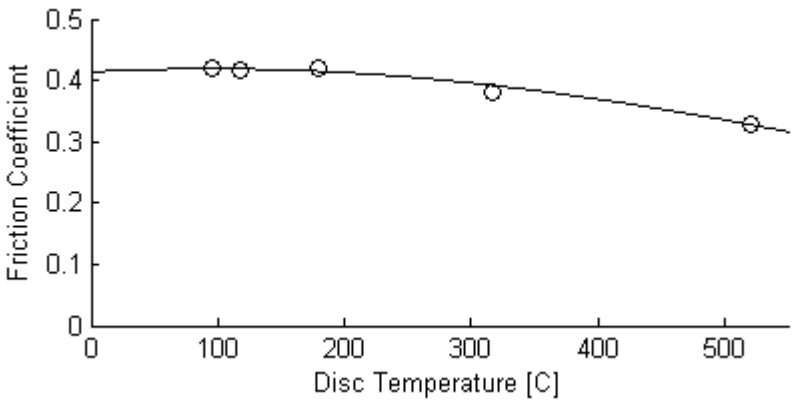

Figure 56. OEM friction coefficient vs. disc temperature.

Just as the EHB brakes, the OEM brakes show a clear dependency on the disc temperature. The friction coefficient drops continuously as the temperature increases. The level of friction is though true to what the manufacturer specified, which was 0.41-0.43 for low to medium temperatures.

As with the EHB pads, no results were found that suggest the friction to be a function of the pressure. Therefore, the standard pads are also said to be dependent on temperature only.

No tests were conducted for the rear OEM brakes, yet again due to the problems with the torque wheel adapters. Contrary to the EHB system, the rear OEM pads can't be

expected to behave similarly to the front OEM pads, since they are not the same material. Until further test can be conducted, the rear OEM friction should be assumed as constant.

6.3.3 Brake temperature model

The heat model of the brake disc and pads is calibrated in the HIL-rig. Logging of all parameters begun before the HIL-rig was powered on. This allows an accurate initial temperature for the brake disc temperature model, since the entire disc should be at room temperature. If the disc was heated up before logging, then only the surface temperature can be recorded by the IR sensor, but the temperature inside the brake disc would be unknown.

6.3.3.1 Disc heat convection

The convection is calibrated using the following procedure.

- The rotational velocity is set to a constant value.
- The brake disc is heated up to 500°C to 600°C by applying manual brake pressure.
- Brake pressure is let off and the disc is left to cool down.
- The procedure is repeated for different rotational velocities to fully capture the velocity dependence of the convection.

Recall Equation 3.7. This equation for the convection has two constants, one that is independent and one that is dependent on the air velocity. The experiment should therefore be done at zero velocity to calibrate the velocity independent constant. However, when rotating, it was noticed that the brake disc was suffering from high disc thickness variation, resulting in a varying temperature. A very low velocity was used instead to calibrate the velocity independent constant.

Figure 57 below shows the correlation between the simulated disc temperature from the heat model and the measured disc temperature.

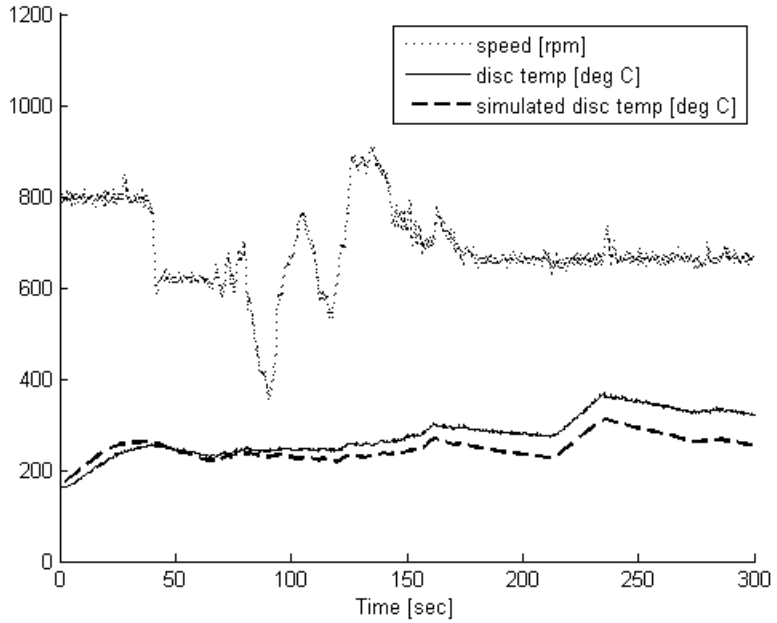

Figure 57. Development of difference between calculated and measured disc temperatures during HIL-rig testing.

Figure 57 shows good simulated temperature throughout the entire test. The input brake torque and speed are both highly transient, yet the simulation did a good job between 25 to 200 seconds. Between 210 and 240 seconds, the temperature increase made the simulation less accurate. With this knowledge, and some of trial and error with the modeling parameters, it was determined that the model can only be accurately tuned for a temperature range of approximately 100°C. The brake pad specific heat and conductivity are highly temperature dependent variables that were entered as constants in the simulation. The specific heat was made a function of temperature and tuned. Figure 58 shows the improved behavior of the model.

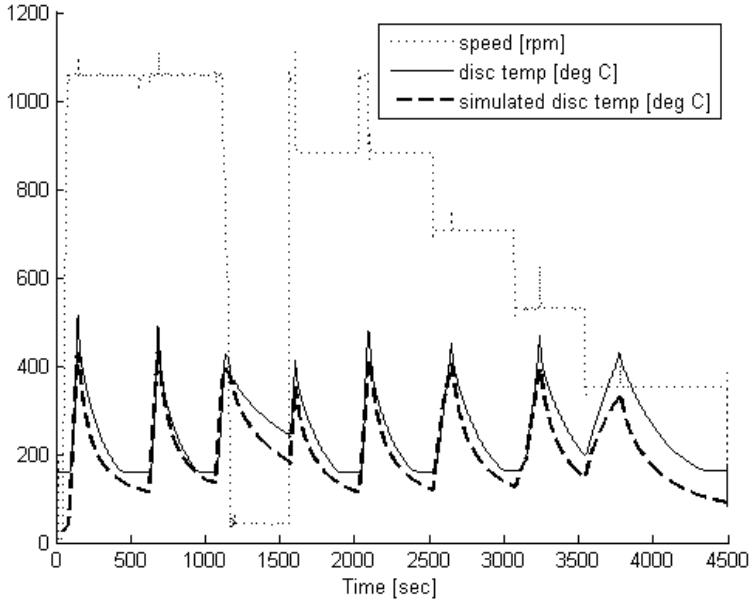

Figure 58. Simulated and measured disc temperatures during HIL-rig testing.

The results in Figure 58 show that simulated disc temperature traces the measured disc temperature well for a much longer time. Note the difference in time scale between Figure 57 and Figure 57.

6.3.3.2 Pad heat model

The pad heat model was not calibrated during HIL-rig testing, since no instrument was installed to record the pad temperature. Note that the tuning of the pad specific heat in section 6.3.3.1 was only aimed at improving the behavior of the brake disc model. To calibrate the imperfect contact factor between the pad and the third body between the disc and the pad, the test executed in chapter 6.3.3.1 should be repeated with a thermocouple installed in the brake pads.

6.3.3.3 Vehicle testing of heat model

The brake heat model was also tested in the final vehicle. This was done to analyze the potential of HIL-rig calibration, since a number of factors differ to the test rig. For instance, the installation environment is more complex, with the standard calipers mounted and wheels surrounding the assembly. Also, the weather conditions come into play. To test the accuracy of the model, the driving cycle described by Figure 59 and Table 3 was used.

Figure 59

Table 3

Location	Description
A	Brake from 120 to 70 kph. Accelerate to 100 kph.
B	Brake from 100 to 70 kph.
C	Brake from 70 to 40 kph. Accelerate to 120 kph at straightaway.

The driving cycle is longer than the one used for calibrating the friction coefficient. This is to analyze the correlation between the calculated and the measures brake temps for longer runs. Also, it is designed to be more similar to a normal road driving scenario. Brake pad and disc temperatures were taken every other lap to give reference data points aside from the starting and final temperatures. The driving cycle was repeated until both pad and disc temps were exceeding 200°C. Then, cooling laps were run where no brakes were applied, until brake temps were below 100°C. Figure 60 shows the results of the testing.

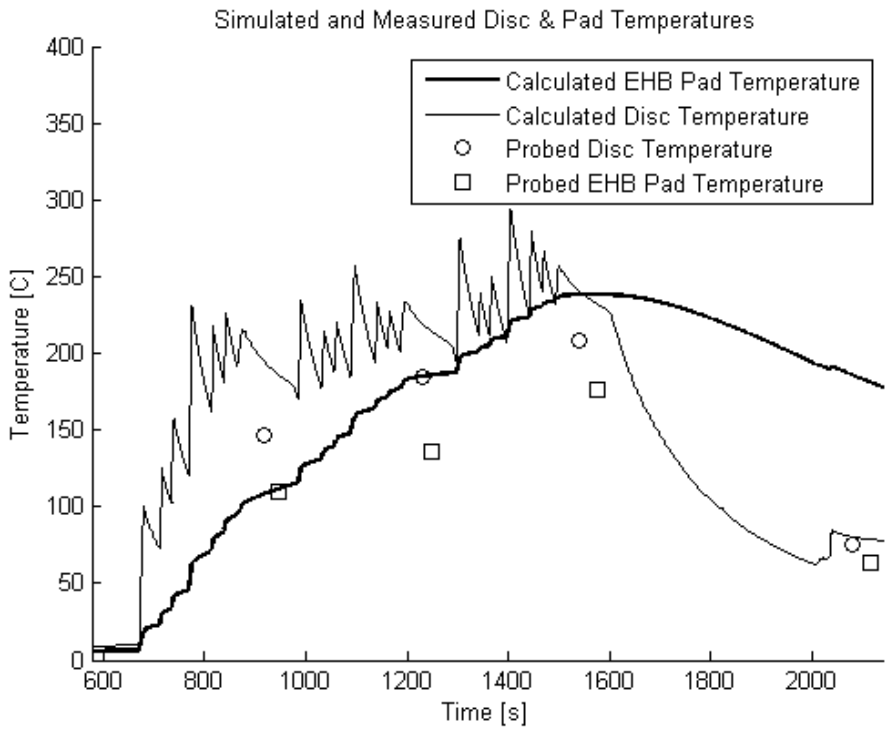

Figure 60. Calculated and measured pad and dics temperatures during vehicle testing

In Figure 60, the solid lines represent the calculated disc and pad temperatures. The circular and square data points are the measured temperatures. The results show that the actual pad temperature is deviating quite drastically from the calculated temperature. The deviation can be attributed to the pad heat buildup not being calibrated during HIL-rig testing. The disc heat model was calibrated on the other hand, and it gives a much better correlation to measured data. The results give an indication on the potential of HIL-rig testing for convenient calibration of software parameters.

6.4 Validation of test vehicle performance

Here, the final performance of the test vehicle is shown. This is done by analyzing the response to a step pressure request, the ability to follow a ramp pressure request and the correlation between requested torque and measured torque for a driving cycle.

Although the aim of the test vehicle is to emulate electric machines, no comparisons between the response and precision characteristics of the EHB system and electric motors are made. The response of an electric motor is highly dependent on the specification and the controller used. Real-world testing is the most reliable source for reference data, but beyond the scope of this thesis. For the EHB, the response is hardware-dependent and therefore not easily altered. By knowing the performance of the test vehicle, the test vehicle user has a reference point for the emulated vehicle system.

6.4.1 Response

The response of the EHB system was analyzed by giving a step pressure request during driving. The step request was given the front left wheel (closest to EHB unit), the rear right wheel (farthest from EHB unit) and all four wheels simultaneously. Steps of 10, 30 and 60 bar for the pressure steps were used. Figure 61 displays the results for a 60 bar pressure step applied at all four corners of the car.

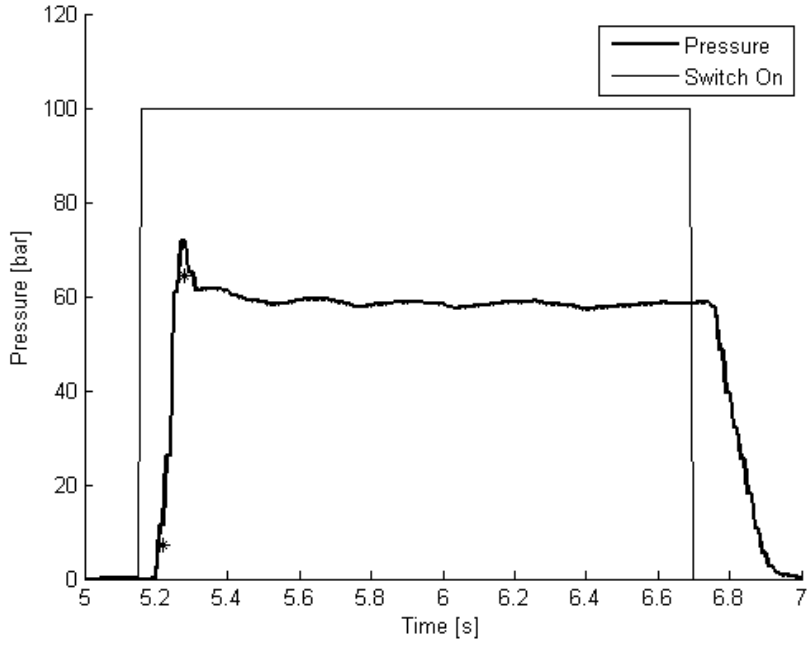

Figure 61. Pressure step response, 60 bar at all four corners.

The response can be defined to be the time between 10% and 90% of the final response value. For this scenario, the response time is 0.06 seconds. However, of interest for the user is also the reaction time from activation of request (shown in Figure 61 as switch on). This adds up another 0.05 seconds to give a total response time of 0.11 seconds.

Of interest for the test vehicle user could also be the response time from a certain pressure to zero pressure. Taking into account the reaction time switch is set to off, this response is close to double the corresponding rise time, at 0.18 seconds.

Aside from plotting the EHB pressure response, the response of the measured wheel torque was also complied. However, doubts about the consistency of the transmission delay did rise when the plots were analyzed. The response times are very short, and any measurement inaccuracy has a big impact on the results. Instead, the response of the vehicle longitudinal acceleration was studied. The data from the accelerometer is recorded without delay. Figure 62 shows the results.

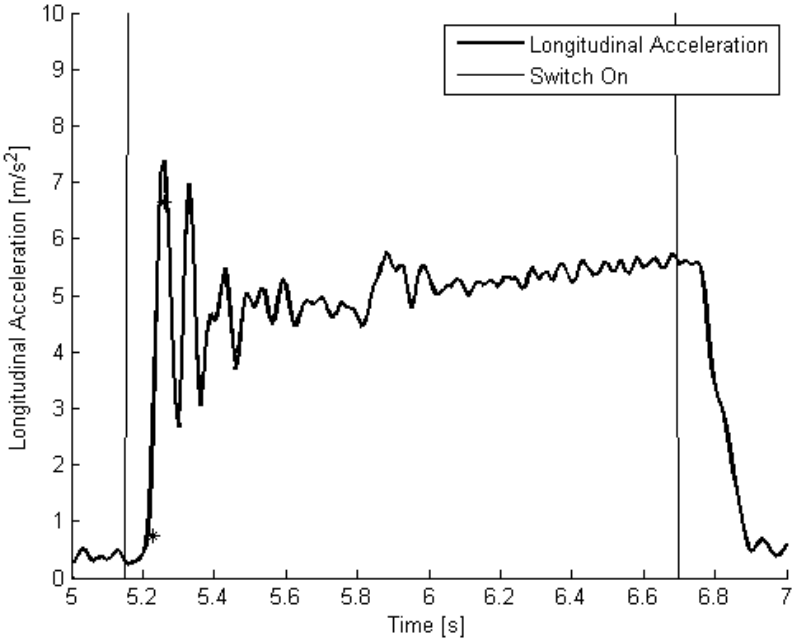

Figure 62. Longitudinal acceleration step response, 60 bar at all four corners.

The response of the vehicle acceleration is very close in magnitude to the pressure response. This indicates that the wheel torque response is likely very close to the EHB pressure response.

6.4.2 Precision to ramp input

The internal pressure regulation of the EHB unit is analyzed using a pressure request ramp. The ramp is set to increase at a rate of 5 bars per second until the vehicle stops. The test is done twice; for one wheel only and for all wheels simultaneously. Figure 63 and Figure 64 show the results of these two runs respectively.

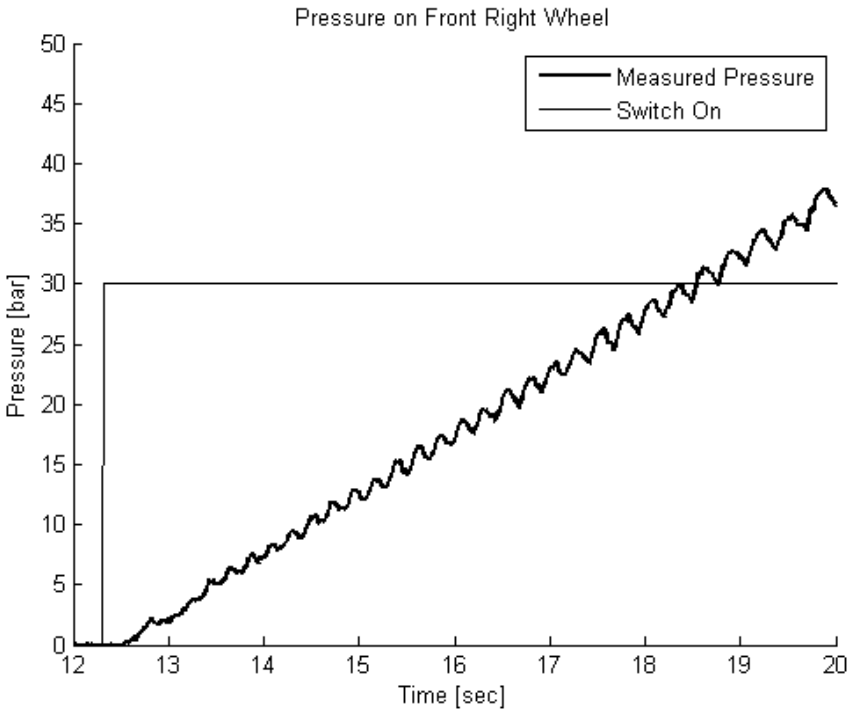

Figure 63. Behavior during ramp up of FR corner pressure.

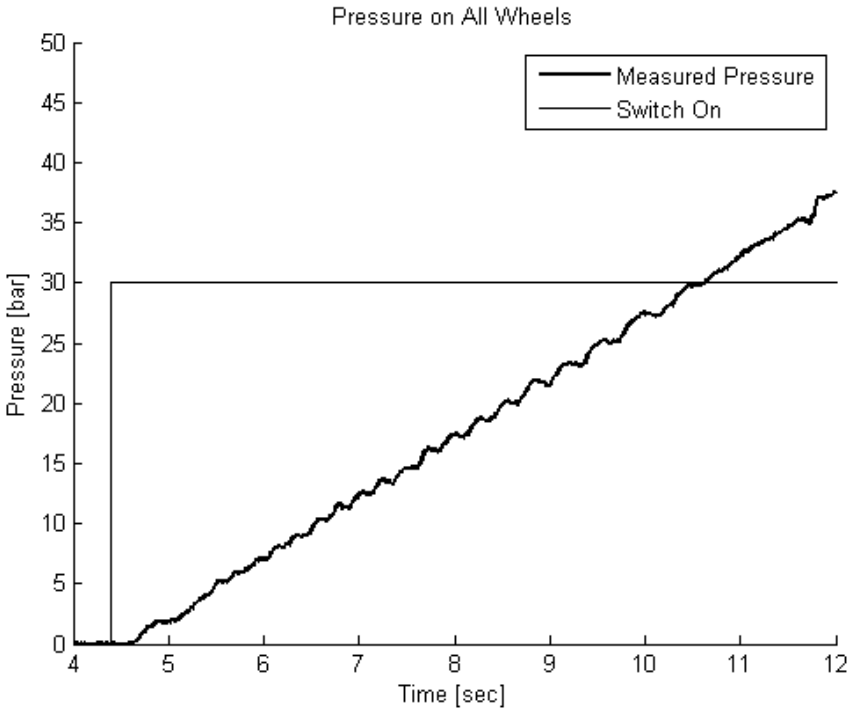

Figure 64. Behavior during ramp up pressure at all four corners.

By examining the results in Figure 63 and Figure 64, the regulation seems a little bit rougher when pressure is applied an individual wheel only. For the first ramp test, the regulation is around ±0.75 bar for high pressure levels. This can be compared to the second ramp test, which exhibits a smoother curve with regulation around ±0.25 bar. For both cases, the precision is best for low levels of pressure. This could be considered a good characteristic, especially for the brake disc cleaning use case.

6.4.3 Precision over driving cycle

To evaluate the precision of the EHB system together with the software models, the same driving cycle as introduced in Section 6.3.3.3 was used. The driving cycle was run with both EHB braking only and OEM braking only. Both cases were repeated with constant friction coefficients (average of friction curves) and with varying friction coefficients (utilizing the brake heat model). From the gathered data, some braking instances are here analyzed. This is done by plotting the graphs of the calculated torque and the measured torque. The error is then calculated as the difference between the curves divided by the measured torque value. The error is plotted in a separate figure.

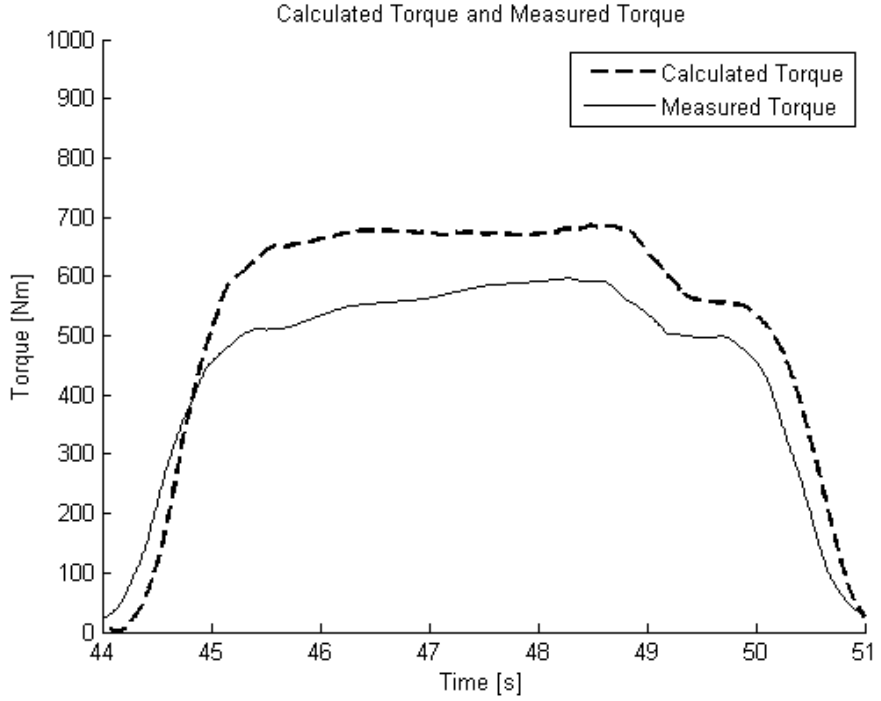

Figure 65. OEM braking with constant friction model.

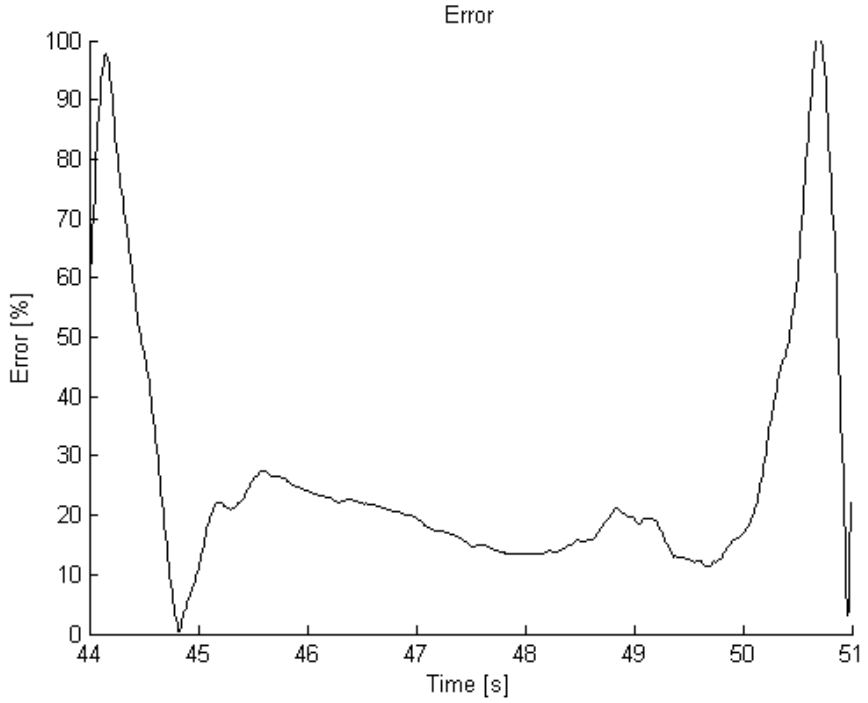

Figure 66. Torque error, OEM braking with constant friction model.

Figures 65 and 66 show the results of a braking scenario with the OEM brakes, using constant friction for the model. The error is between 50-100 Nm or 15-25%.

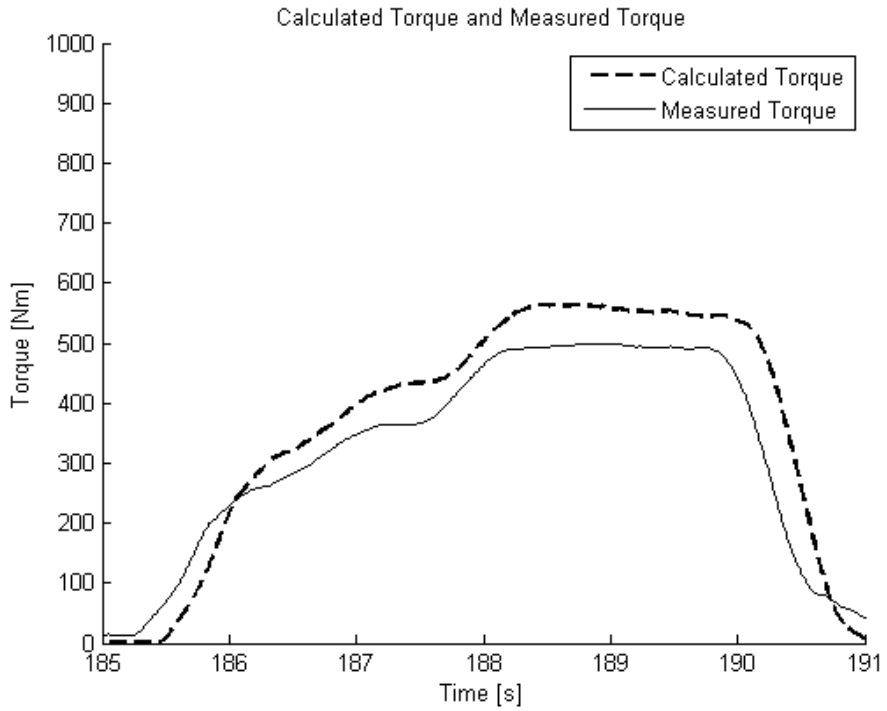

Figure 67. EHB braking with constant friction model.

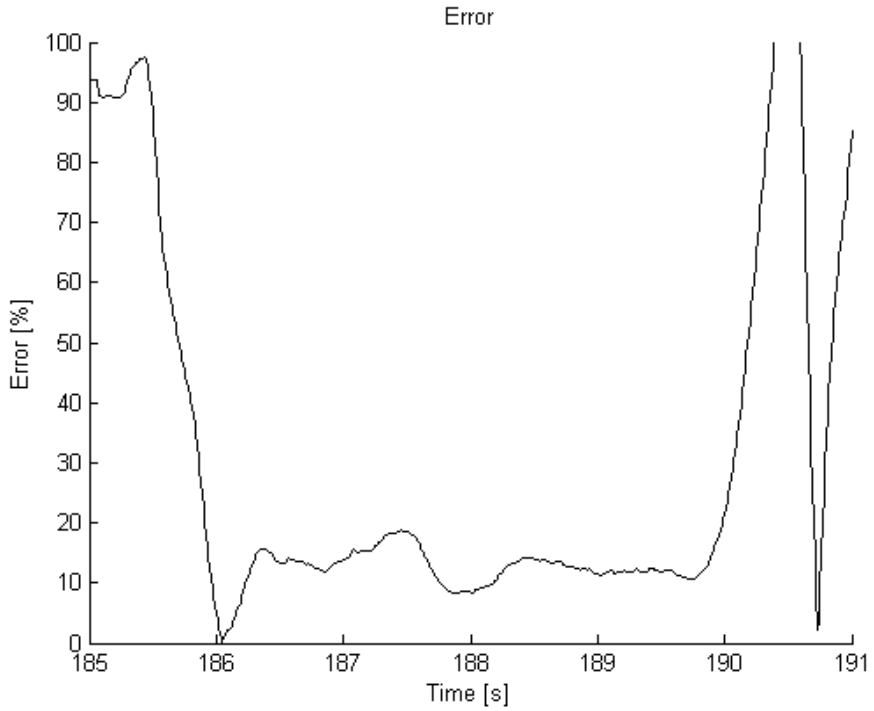

Figure 68. Error, EHB braking with constant friction model.

Figures 67 and 68 show the results of a braking scenario with the EHB brakes, using constant friction for the model. The error is between 40-80 Nm or 8-15%.

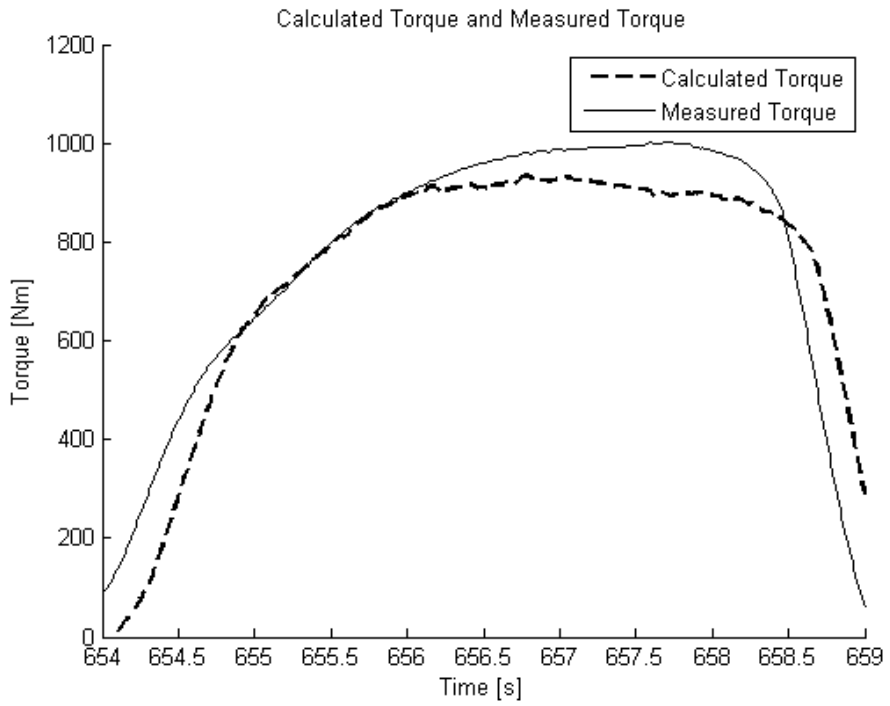

Figure 69. OEM braking with temperature-dependent friction.

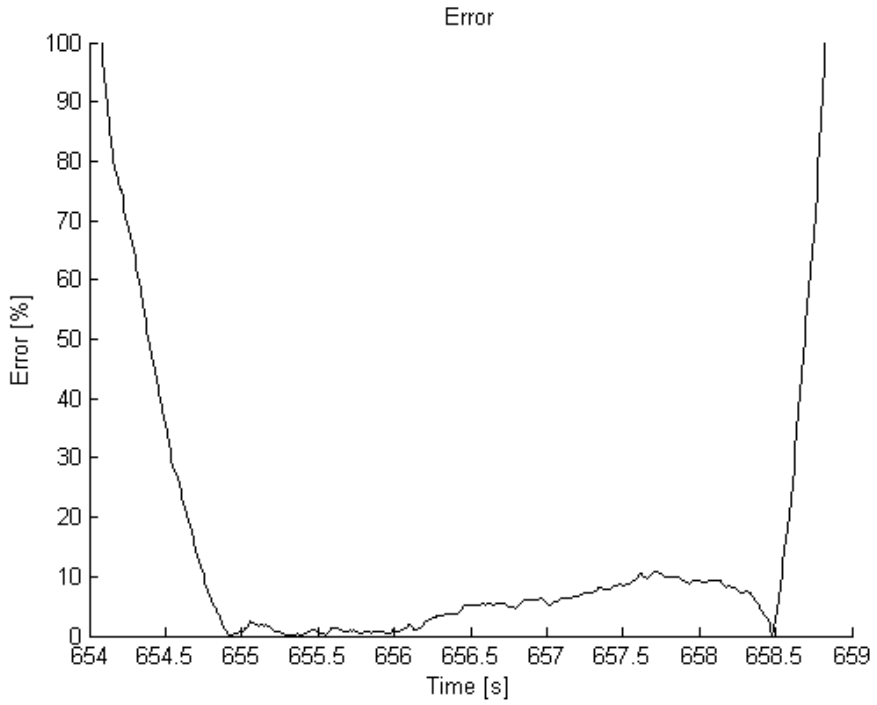

Figure 70. Error, OEM braking with temperature-dependent friction.

Figures 69 and 70 show the results of a braking scenario with the OEM brakes, using the temperature-dependent friction and the heat model. The error is constantly below 10%.

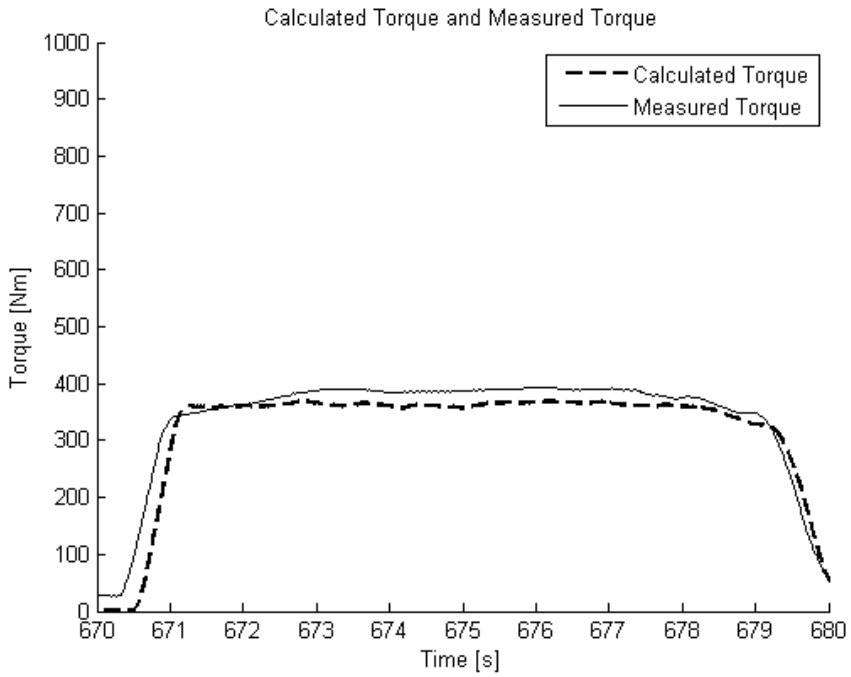

Figure 71. EHB braking with temperature-dependent friction.

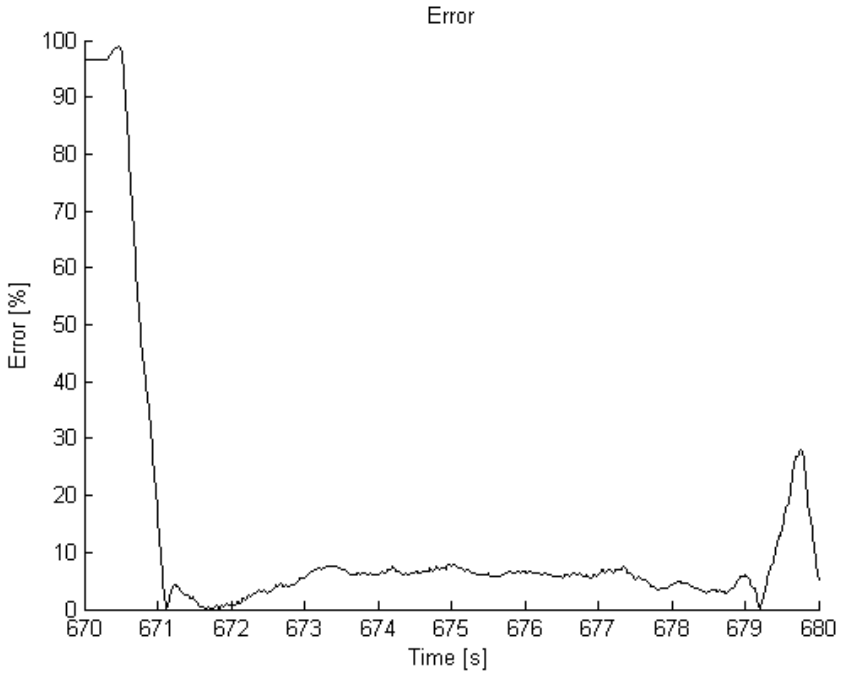

Figure 72. Error, EHB braking with temperature-dependent friction.

Figures 71 and 72 show the results of a braking scenario with the EHB brakes, using the temperature-dependent friction and the heat model. The error is constantly below 8%.

Overall, the data from the driving tests shows that the measured torque consistently matches up better with the simulation when using the model and varying friction coefficients. Still, the user should expect around 10% deviation in realized torque compared to desired torque.

6.5 Notes from test driving

During testing, a transient behavior of the friction coefficient of both the EHB and the OEM brake pads was observed. That is to say, a constant torque request would give a wheel torque that deviated either linearly or exponentially from the intended value. To capture this transient behavior in the software models, further HIL-rig calibration of the brake heat model is required. Of main concern is the temperature buildup and cool-down of the brake pads. With more insight in the brake disc-pad thermodynamic interaction, the precision of the EHB system might be improved.

Recall the temperature-dependence of the specific heat and conductivity of the EHB pads, shown in Figure 41. This quite drastic behavior was confirmed during testing. The EHB brakes require hard use to exceed 200°C. Overall, the pads give a very predictable temperature development of the complete disc/pad system.

On the contrary, the OEM pads do get heated up quite quickly. The disc temperature increases quicker too when using the OEM brakes hard. For the additive regen braking use case, when the OEM brakes are mainly used, the brake temperatures should be measured continuously.

The method for taking the brake temperatures could be improved to give better readings in the future. For the pads, a shallow measurement hole can be drilled to make sure that the temperature is taken at the same location each time. Also, this decreases the effect of the surrounding air, since a larger portion of the thermocouple is surrounded by pad material.

7 Example Use Case

To sum up the master thesis, a strategy for additive regen braking is analyzed using the test vehicle. This use case is chosen as an example, since it enables all developed software models to be utilized.

The idea behind the regen strategy is simple; the amount of added regen braking should be directly proportional to the amount of OEM braking. To achieve this, recall the brake demand module of Chapter 4.4. This is modified slightly, giving the layout described by Figure 73.

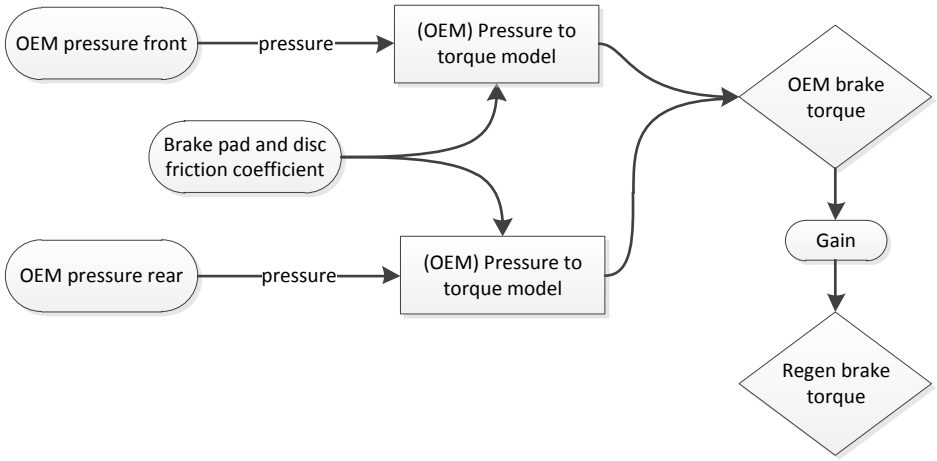

Figure 73. Layout of additive use case brake demand module.

The OEM brake torque is multiplied by a user-defined constant, giving the desired amount of regen brake torque. Note that the OEM brake torque calculation is always present in this software module, and that only minor modifications are required to achieve the intended functionality.

To further describe the functionality, the OEM brake pressure vs. brake pedal travel curve was mapped in the test vehicle. The array of values was then put through Equation 3.1 to give a wheel brake torque vs. brake pedal travel curve for the OEM system. Multiplying this curve by a constant gives a new curve. Both graphs are shown in Figure 74.

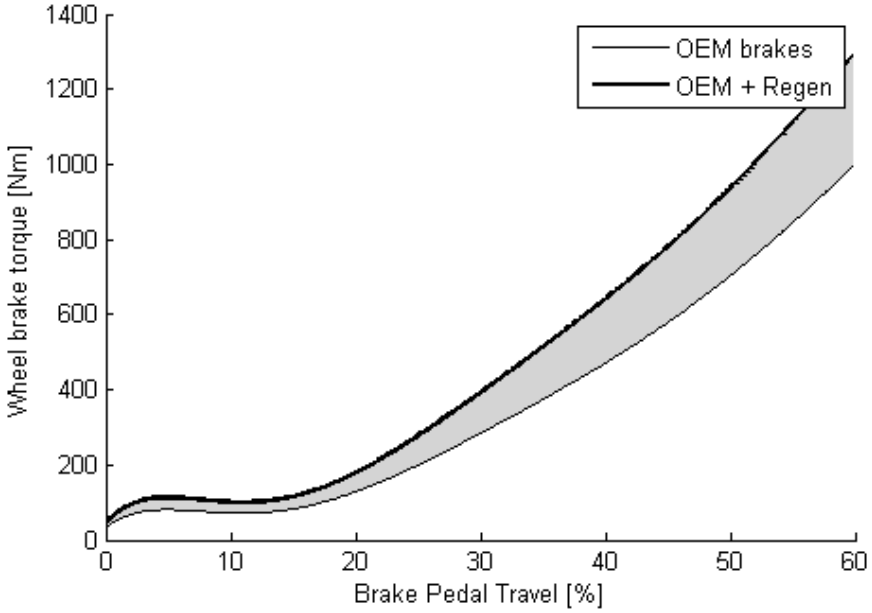

Figure 74. Wheel brake torque vs. brake pedal travel for OEM and OEM+Regen.

The grey-shaded area between the shown curves is the amount of regen braking that should be done. The figure also gives a good idea of pedal feel of the OEM system. A potential area for implementation of additive braking is clearly the early part of the pedal travel. However, increasing the step-in brake torque too much gives a brake system that is difficult to modulate, for instance when coming to a stop.

For testing, the added regen braking torque was chosen to be 40% of the OEM torque. The test vehicle was then driven around the test circuit at varying speeds and braking levels, in an attempt to capture many possible braking scenarios that can arise when travelling on public roads. Figure 75 shows the velocity of the test vehicle during the test.

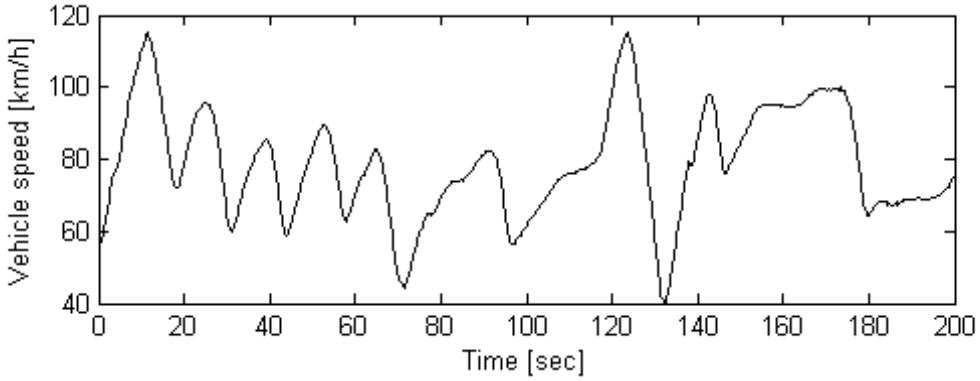

Figure 75. Profile of vehicle speed during use case test.

From the software motor model, the simulated motor state can be recorded. By plotting all data points of motor torque and motor speed, Figure 76 is created.

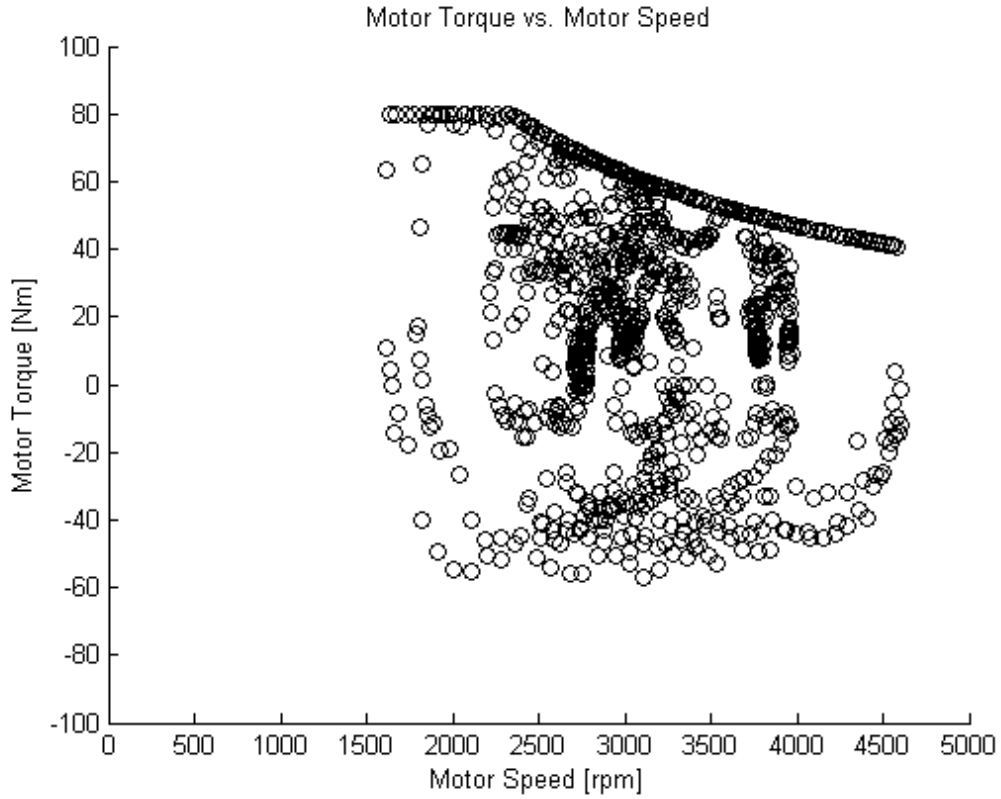

Figure 76. Motor torque vs motor speed for use case test.

Figure 76 shows that the motor is working in both propulsion and regen mode. It is also possible to conclude that the motor is reaching its limit during propulsion more frequently than during regeneration.

It is also possible to record the battery state. In Figure 77, the state of charge of the battery is plot over time.

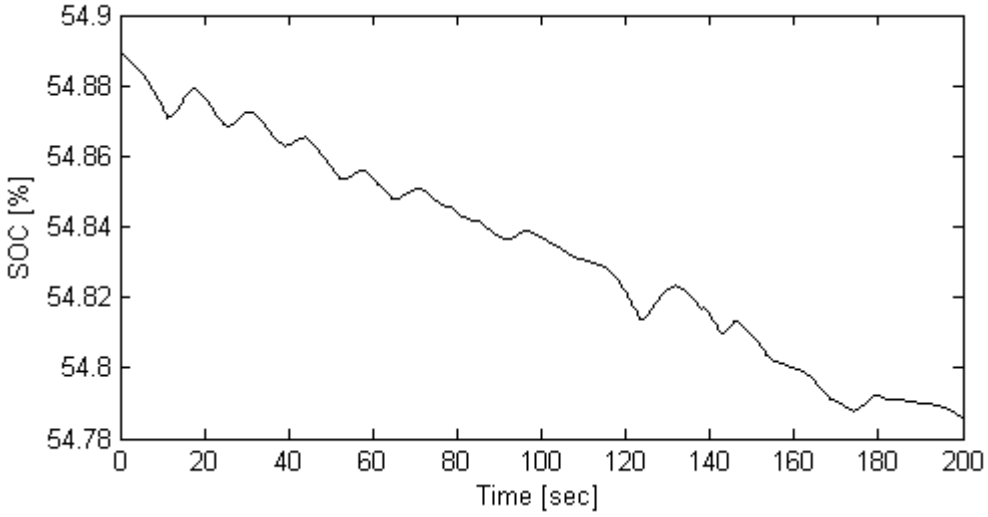

Figure 77. State of charge of battery during use case test.

The battery is both discharged and recharged during the test. The overall change in state of charge during this driving scenario is negative, although quite small.

In Figure 78, two particular braking instances are displayed. The figure shows the brake pedal travel (black line) and vehicle longitudinal acceleration (grey line).

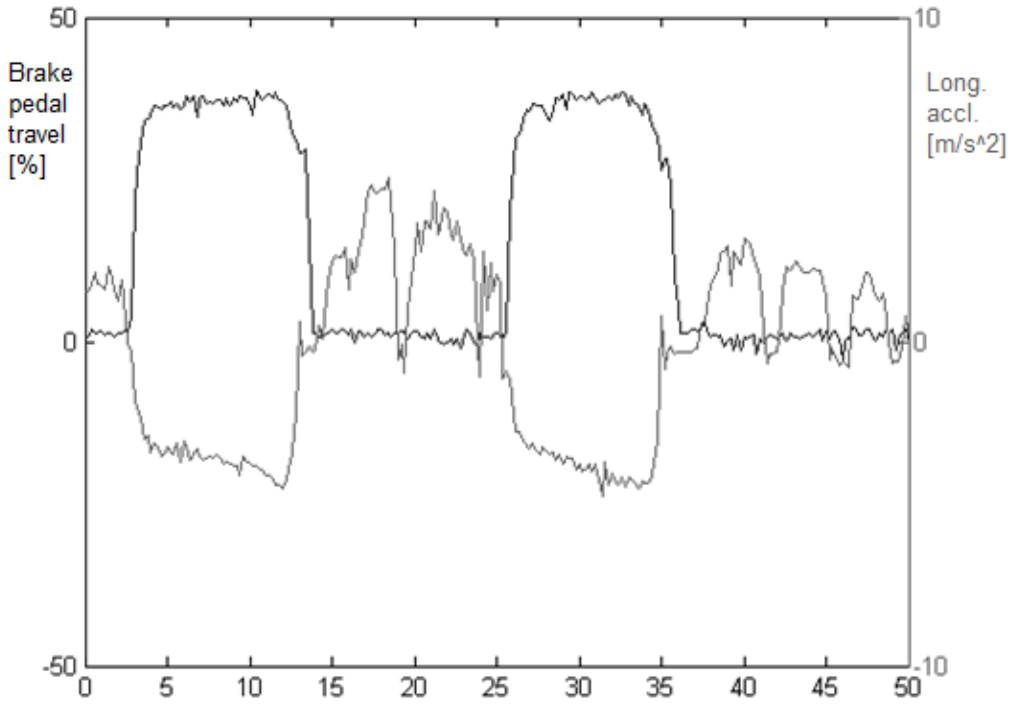

Figure 78. Brake pedal travel and longitudinal acceleration during two braking instances.

The deceleration is quite consistent with the brake pedal input during the two braking situations in Figure 78. The graph indicates that the brake demand model is working smoothly, which was also the subjective impression of the test driver. Also, the brake pedal felt more direct while still being easy to modulate.

The study on the energy-saving potential and the effect on the pedal feel facilitates the assessment of the additive regen braking function. However, the effect on the vehicle stability should also be taken into account. This undertaking was though beyond the scope of this example case study.

8 Conclusions

Looking at the results from Chapters 6 and 7, the following conclusions can be drawn:

- The friction coefficient of both vehicle brake systems were shown to be a function of temperature. During braking, there's a transient behavior for the friction coefficient currently not captured by the brake model.
- The disc heat model was calibrated in the HIL-rig and correlated well to measurement done with the final test vehicle in real-world conditions. The pad heat model was not calibrated and did not correlate well to measurements from the test track. The heat model coupled with the temperature dependent friction coefficient was proved to improve the correlation between calculated and measured wheel torque during braking, compared to when using a constant friction coefficient.
- The step response for the EHB system was presented. The EHB builds up brake line pressure quicker than it decreases the pressure. This is due to the brake fluid return hose to the reservoir being too small in diameter. The precision during a pressure request ramp was shown. The EHB is more precise when regulating all four brakes compared to when regulating an individual brake. More testing needs to be done to find an explanation.
- The presented EHB system performance was not compared to the performance of an electric driveline. Reference real-world data should be gathered from an electric test vehicle.
- An example use case was conducted. It showed how the different aspects of additive regen braking can be analyzed using the test vehicle. The example use case displayed realistic behavior from motor and battery models.

9 Future Work

To gain better EHB performance, further development of the brake heat model is recommended. This necessitates the implementation of a thermocouple in the brake HIL-rig to better understand the thermodynamic behavior of the brake pads. To make data sampling in the test vehicle easier, thermocouples and IR-sensors can be installed to monitor brake and disc temperatures respectively.

The friction coefficient variation over temperature of the rear EHB and OEM brakes should be determined using the same procedure as the one used for the front axle. The rear EHB system pads are the same as for the front, so they can be expected to behave similarly to the front brakes. However, the rear OEM system pads are not the same material as the front OEM pads, so they might display slightly different properties.

Future work naturally includes putting the test vehicle into use. That is to say, let engineers apply their models in the vehicle. Running the test car will reveal more attributes of the vehicle than shown in this study, such as long-term reliability, flexibility of software and overall ease-of-use. At its current state, the car can very well be used for basic function testing and clinic studies.

Reference testing of an electric vehicle should be conducted if knowledge of the relative brake performance of the EHB system compared to an actual electric driveline is vital. The brake response time of an electric vehicle can be measured either monitoring its longitudinal acceleration or by using the torque wheels.

Using the experiences gained from the test sessions conducted, control functions of the production cars can be developed. This may lead to more efficient, safe and reliable embedded vehicle systems.

10 References

Andersson, M, et al. "Road Friction Estimation, IVSS Project Report." 2009.

BBC news. http://news.bbc.co.uk/2/hi/business/8497471.stm. February 2010.

Blundell, Michael and Damian Harty. Multibody Systems Approach To Vehicle Dynamics. Elsevier Science & Technology, 2004.

Coelingh, Erik, Pascal Chaumette and Mats Andersson. "Open-Interface Definitions for Automotive Systems Application to a Brake by Wire System." 2002.

Day, Andrew J, Hon Ping Ho and Khalid Hussain. "Brake System Simulation to Predict Brake Pedal Feel in a Passenger Car." 2009.

de Arruda Pereira, Joaquim A. "New Fiesta: Brake Pedal Feeling Development to Improve Customer Satisfaction." 2003.

Elert, Glenn. The Physics Hypertextbook. 1998. December 2010 <http://physics.info>.

Hancock, Matthew and Francis Assadian. "Impact of Regenerative Braking on Vehicle Stability." 2007.

Hoffman, Lars. Electric Motor Drives Horace Ka Ho Lai and David Madås. 14 October 2010.

Hopkins, Brad, Saied Taheri and Mehdi Ahmadian. "Yaw Stability Control and Emergency Roll Control for Vehicle Rollover Mitigation." 2010.

Hoseinnezhad, Reza and Alireza Bab-Hadiashar. "Recent Patents on Measurement and Estimation in Brake-By-Wire." 2008.

Hughes, Austin. Electric Motors and Drives. Oxford: Elsevier Ltd., 2006.

IBT Power Ltd. Lithium Ion Technical Data. 2011. <http://www.ibt-power.com/Battery_packs/Li_Ion/Lithium_ion_tech.html>.

Milliken, William F and Douglas L Milliken. Race Car Vehicle Dynamics. Milliken Research Associates, 1995.

Olsson, Gunnar, et al. Use case definition meeting David Madås and Horace Lai. December 2010.

Pascali, Leonardo, et al. "Customer Orientation: A Further Target in Brake System Design." 2003.

Rajesh, A T, Bisen Badal and Sharad Pol. "Co-relating Subjective and Objective Brake Performance: A Case Study." 2006.

Shim, Taehyun and Donald Margolis. "Using μ Feedforward for Vehicle Stability Enhancement." n.d.

Talati, Faramarz and Salman Jalalifar. "Analysis of heat conduction in a disk brake system." 2009.

Wicks, Frank and Kyle Donnelly. "Modeling Regenerative Braking and Storage for Vehicles." 1999.

von Albrichsfeld, Christian and Jürgen Karner. "Brake System for Hybrid and Electric Vehicles." 2009.